NATIONAL ADVISORY COMMITTEE FOR AERONAUTICS

TECHNICAL NOTE

No. 1574

WIND-TUNNEL INVESTIGATION OF THE BOUNDARY LAYER ON AN NACA 0009 AIRFOIL HAVING 0.25- AND 0.50-AIRFOIL CHORD PLAIN SEALED FLAPS

By Jack D. Brewer and Josephine F. Polhamus

Langley Memorial Aeronautical Laboratory
Langley Field, Va.

Washington
April 1948

NATIONAL ADVISORY COMMITTEE FOR AERONAUTICS

TECHNICAL NOTE NO. 1574

WIND-TUNNEL INVESTIGATION OF THE BOUNDARY LAYER ON AN NACA 0009 AIRFOIL HAVING 0.25- AND 0.50-AIRFOIL CHORD PLAIN SEALED FLAPS

By Jack D. Brewer and Josephine F. Polhamus

SUMMARY

An investigation was conducted to determine the boundary-layer characteristics of an NACA 0009 airfoil equipped with 0.25- and 0.50-airfoil chord plain sealed flaps. The tests were made to define as thoroughly as possible the characteristics of two of the configurations used in a comprehensive investigation of control-surface characteristics and also to provide additional data for comparison with previous boundary-layer analyses.

The measured velocity profiles and the boundary-layer parameters determined from them are presented.

INTRODUCTION

An extensive investigation of control-surface characteristics has been conducted in the Langley 4- by 6-foot vertical tunnel. The greater part of the investigation consisted of two-dimensional tests of an NACA 0009 airfoil with various flap arrangements. Pressure-distributions of some of the models are presented in references 1 to 3. Most of the force and moment measurements have been summarized in reference 4.

In the present investigation measurements were made of the boundary-layer characteristics of an NACA 0009 airfoil having 0.25- and 0.50-airfoil chord plain sealed flaps. Results of force and moment tests of the same model are reported in reference 5. The tests were made to define as completely as possible the characteristics of two representative airfoil-flap configurations under the specific test conditions of the general control-surface investigation.

A previous boundary-layer investigation (reference 6) indicated that measured boundary-layer parameters did not agree with calculated boundary-layer parameters behind the control-surface hinge line. The boundary-layer measurements of this investigation are intended for use in obtaining a more accurate method for predicting the boundary layer in the region of the trailing edge from which prediction a correlation of measured hinge moments and calculated boundary-layer parameters might then be developed.

SYMBOLS

c airfoil chord

c_f flap chord

x distance along chord

y distance perpendicular to surface

q_o free-stream dynamic pressure outside boundary layer $\left(\frac{\rho}{2} U_o^2\right)$

U_o free-stream velocity

U velocity at outer edge of boundary layer

u velocity within boundary layer

δ^* boundary-layer displacement thickness $\left[\int_0^\infty \left(1 - \frac{u}{U}\right) dy\right]$

θ boundary-layer momentum thickness $\left[\int_0^\infty \frac{u}{U}\left(1 - \frac{u}{U}\right) dy\right]$

H boundary-layer shape parameter (δ^*/θ)

K ratio of velocity at edge of boundary layer to free-stream velocity (U/U_o)

δ_f flap deflection

α_o angle of attack for airfoil of infinite aspect ratio with subscript u for uncorrected value

APPARATUS AND MODEL

The present investigation was conducted in the Langley 4- by 6-foot vertical tunnel (described in reference 7 and modified as related in reference 2). The model, constructed of laminated mahogony to the NACA 0009 profile, had a chord of 2 feet and completely spanned the test section. It was equipped with plain sealed flaps having chords of 25 percent and 50 percent of the airfoil chord.

Ordinates for the airfoil are given in table I. Dimensions of the model are given in figure 1.

Boundary-layer profiles were measured by means of two pressure "mice," one mounted on the upper and one on the lower surface of the model. Each "mouse" consisted of 14 total-pressure tubes and 2 static-pressure tubes. Each of the mice tubes was calibrated against a standard tube.

TEST PROCEDURE

The tests were made at an average dynamic pressure of 16.2 pounds per square foot, which, for standard atmospheric conditions, corresponds to an airspeed of approximately 79.6 miles per hour and to a test Reynolds number of approximately 1.49×10^6, based on the 2-foot chord. The turbulence factor for the Langley 4- by 6-foot vertical tunnel is 1.93.

For the present investigation the model was tested as though only one flap existed at a time. (See fig. 1.) The nose gap of the flap not in use was completely filled with plasticine and faired to the airfoil contour. The gap of the flap being investigated was sealed by a small amount of plasticine placed only at the nose of the flap. Measurements were made for positive deflections only but, because mice were located on both the upper and lower surfaces and because the model was symmetrical, values for equivalent negative flap deflections can be obtained.

The total pressure and static pressure were measured relative to the total pressure in the free stream. Positions of the tubes above the surface were measured to the nearest 1/128 inch.

CORRECTIONS

Tunnel corrections were applied to the angle of attack by an extension of the method presented in reference 8. The equations used were as follows: For the 0.25c flap,

$$\alpha_{o_u} = 1.023\alpha_{o_u} + 0.0031\delta_f$$

For the 0.50c flap,

$$\alpha_o = 1.023\alpha_{o_u} + 0.0110\delta_f$$

A correction for the effective center location, given in reference 9, was applied to the mice-tube heights.

RESULTS

Boundary-layer velocity profiles for various stations along the airfoil chord are presented in figures 2 to 8 for given flap conditions. The velocity profiles shown are based on the velocity at the outer edge of the boundary layer U. Conversion to profiles based on the free-stream velocity can be obtained by multiplying the given velocity ratios by the factor K presented on the figures. The factor $\left(K = \frac{U}{U_o}\right)$ is related to the pressure coefficient approximately by the equation:

$$K = (1 - P)^{1/2}$$

where

$$P = \frac{p - p_o}{q_o}$$

and

p = static pressure at a point on airfoil

p_o = static pressure in free air stream

Some of the test points have been omitted from the figures in order to make the curves more legible.

In figures 9 to 15, the boundary-layer displacement-thickness parameter δ^*/c, the momentum-thickness parameter θ/c, and the shape parameter H are plotted against corrected angle of attack for various stations along the airfoil. Consistent scales could not be used throughout the figures because of the wide variations in the values of the parameters. The values of H on the upper surface at the 0.25c station are fairly large at most negative angles of attack. This condition indicates a laminar boundary layer as far back as that station at those angles of attack. Falkner (references 10 and 11) indicates that values of H for a laminar boundary layer should be substantially higher than those shown in these figures (at the higher negative angles of attack), but as yet no explanation of the discrepancy has been found. The sudden break in the curve (at approximately 0° for 0° flap deflection δ_f and at more negative angles of attack as the flap is deflected) and the comparatively low values of H in the positive range of angle of attack indicate transition to turbulent flow. At the 0.46c station and at stations further aft, transition has already occurred throughout the angle-of-attack range. These observations are substantiated by the velocity profiles. As the angle of attack is increased, the rapid increase in the value of H near the trailing edge on the upper surface indicates an approach to separation. The shape parameter increases to over 2.4 at the trailing edge with the 0.25c flap deflected 10° (fig. 12(c)) and becomes even larger with the 0.50c flap deflection. (See fig. 15(c).) Reference 12 predicts turbulent separation at values of H between 1.8 and 2.6 but in no case is final separation shown by the present velocity-profile results. It is possible, therefore, that the mouse tubes near the surface, which measure an average flow, will not always indicate when separation occurs.

An indication of the variation of δ^*/c, θ/c, and H with δ_f can be obtained from figure 16. The data are presented for various angles of attack, for the upper surface, and for only one station ($x = 0.95c$). Values for negative flap deflections are actually values for conditions on the lower surface at positive flap deflections. The discrepancies at zero angle of attack are probably caused by construction irregularities, nonuniform surface conditions, or misalinement of the air stream. Similar plots for the other stations can be obtained from the data of figures 9 to 15.

Figures 17 and 18 present plots of u/U against H for the two flaps tested, for various angle-of-attack and flap-deflection conditions, and for two values of y/θ. Curves from figure 9 of reference 12, obtained from a large amount of turbulent boundary layer data on various plain airfoils, are presented for comparison with the data of the present paper. The present data for an airfoil with sealed flaps deflected up to 10° substantiate the conclusion of reference 12 that, for turbulent boundary layers, u/U is a function of H alone for a given value of y/θ.

CONCLUDING REMARKS

A boundary-layer investigation has been conducted in the Langley 4- by 6-foot vertical tunnel on an NACA 0009 airfoil having 0.25- and 0.50-airfoil-chord plain sealed flaps. The purpose of the tests was to determine the characteristics of two of the configurations used in a comprehensive control-surface investigation as completely as possible and also to provide data for comparison with previous boundary-layer results. The data may be useful for various analyses, especially for a possible hinge-moment correlation. Because of the high turbulence level of the Langley 4- by 6-foot tunnel, however, it is suggested that only data obtained in the same tunnel at the same Reynolds number be used in any analysis involving these results.

The measured velocity profiles and the boundary-layer parameters determined from them are presented.

Langley Memorial Aeronautical Laboratory
National Advisory Committee for Aeronautics
Langley Field, Va., December 23, 1947

REFERENCES

1. Street, William G., and Ames, Milton B., Jr.: Pressure-Distribution Investigation of an N.A.C.A. 0009 Airfoil with a 50-Percent-Chord Plain Flap and Three Tabs. NACA TN No. 734, 1939.

2. Ames, Milton B., Jr., and Sears, Richard I.: Pressure-Distribution Investigation of an N.A.C.A. 0009 Airfoil with a 30-Percent-Chord Plain Flap and Three Tabs. NACA TN No. 759, 1940.

3. Ames, Milton B., Jr., and Sears, Richard I.: Pressure-Distribution Investigation of an N.A.C.A. 0009 Airfoil with an 80-Percent-Chord Plain Flap and Three Tabs. NACA TN No. 761, 1940.

4. Sears, Richard I.: Wind-Tunnel Data on the Aerodynamic Characteristics of Airplane Control Surfaces. NACA ACR No. 3L08, 1943.

5. Spearman, M. Leroy: Wind-Tunnel Investigation of an NACA 0009 Airfoil with 0.25- and 0.50-Airfoil-Chord Plain Flaps Tested Independently and in Combination. NACA TN No. 1517, 1947.

6. Mendelsohn, Robert A.: Wind-Tunnel Investigation of the Boundary Layer and Wake and Their Relation to Airfoil Characteristics - NACA 65_1-012 Airfoil with a True Contour Flap and a Beveled-Trailing-Edge Flap. NACA TN No. 1304, 1947.

7. Wenzinger, Carl J., and Harris, Thomas A.: The Vertical Wind Tunnel of the National Advisory Committee for Aeronautics. NACA Rep. No. 387, 1931.

8. Glauert, H.: Wind Tunnel Interference on Wings, Bodies and Airscrews. R. & M. No. 1566, British A.R.C., 1933.

9. Young, A. D., and Maas, J. N.: The Behaviour of a Pitot Tube in a Transverse Total-Pressure Gradient. R. & M. No. 1770, British A.R.C., 1937.

10. Falkner, V. M.: A Further Investigation of Solutions of the Boundary Layer Equations. R. & M. No. 1884, British A.R.C., 1937.

11. Falkner, V. M.: Simplified Calculation of the Laminar Boundary Layer. R. & M. No. 1895, British A.R.C., 1941.

12. von Doenhoff, Albert E., and Tetervin, Neal: Determination of General Relations for the Behavior of Turbulent Boundary Layers. NACA ACR No. 3G13, 1943.

TABLE I

ORDINATES FOR NACA 0009 AIRFOIL

[Stations and ordinates in percent of airfoil chord]

Station	Ordinate
0	0
1.25	1.42
2.50	1.96
5.0	2.67
7.5	3.15
10	3.51
15	4.01
20	4.30
25	4.47
30	4.50
40	4.35
50	3.97
60	3.42
70	2.75
80	1.97
90	1.09
95	.61
100	.10
L. E. radius: 0.89	

NACA

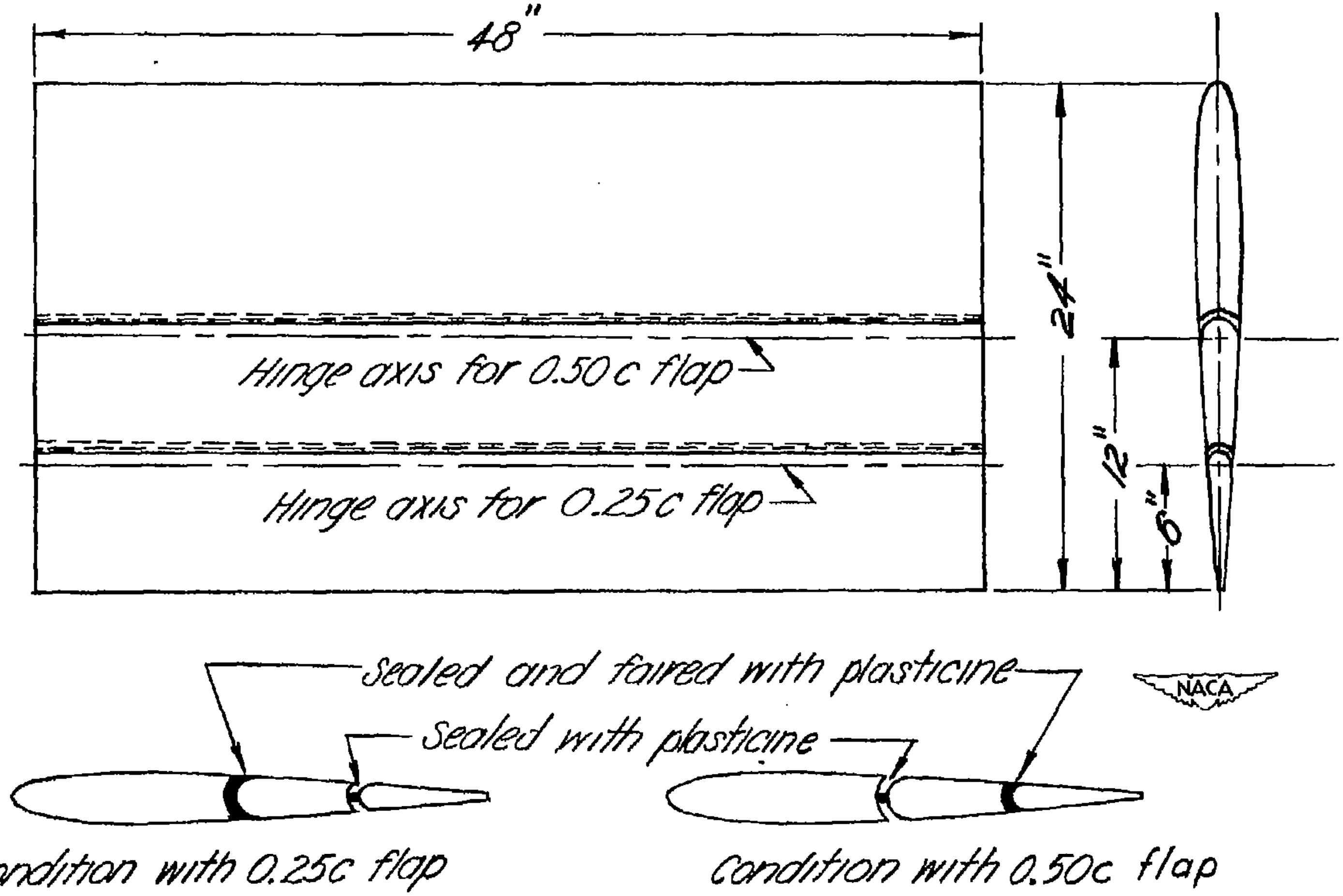

Figure 1.-Details of NACA 0009 model having 0.25c and 0.50c plain sealed flaps.

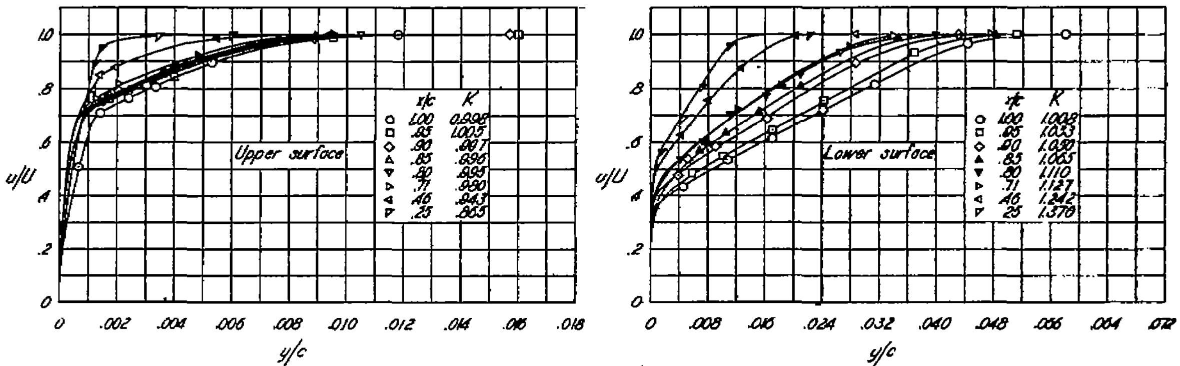

(a) $\alpha_0 = -10.2°$

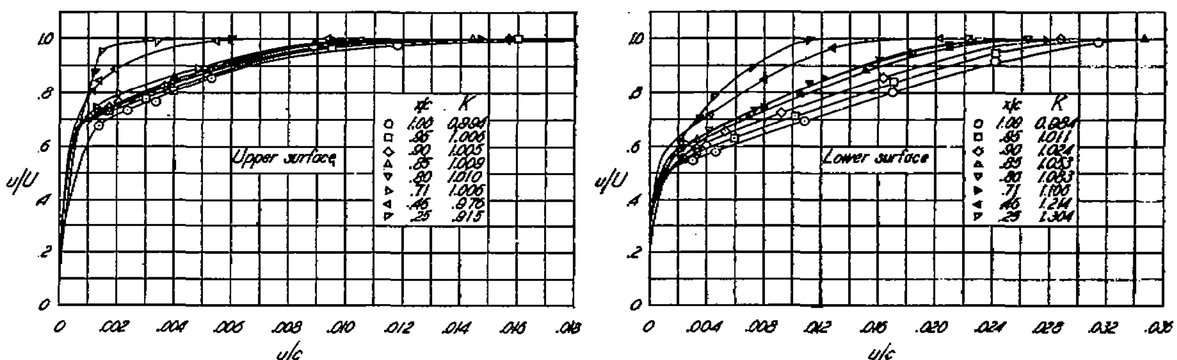

(b) $\alpha_0 = -8.2°$

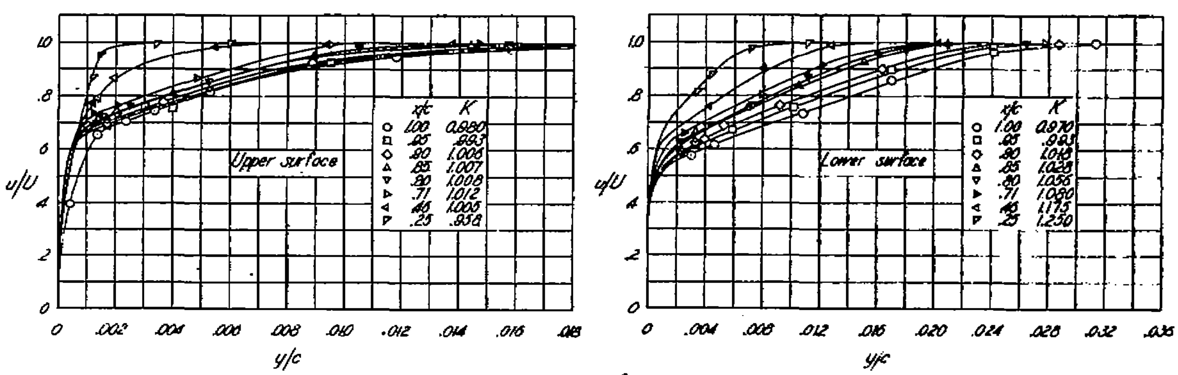

(c) $\alpha_0 = -6.1°$

Figure 2.- Boundary-layer velocity profiles on NACA 0009 airfoil.

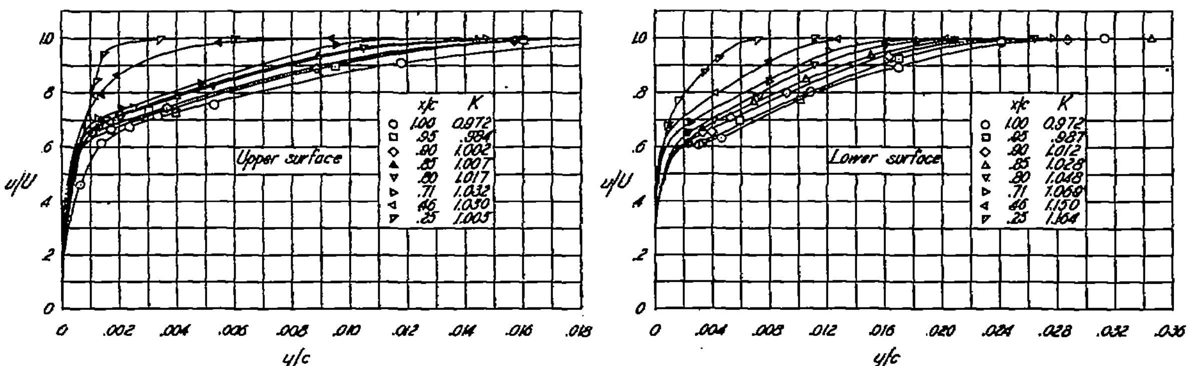

(d) $\alpha_0 = -4.1°$

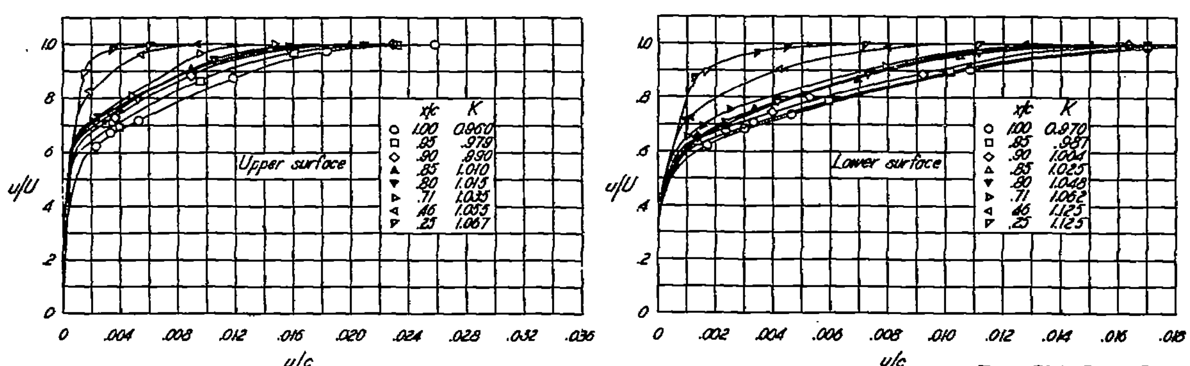

(e) $\alpha_0 = -2.0°$

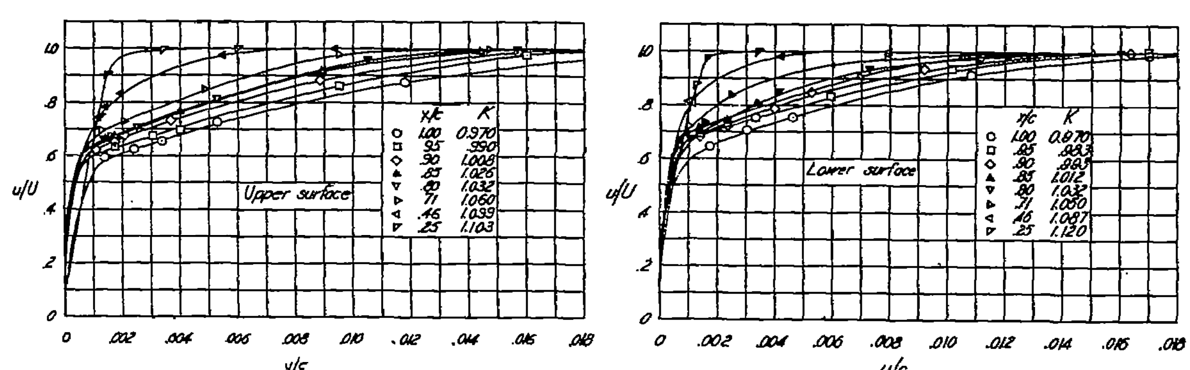

(f) $\alpha_0 = 0°$

Figure 2.– Continued.

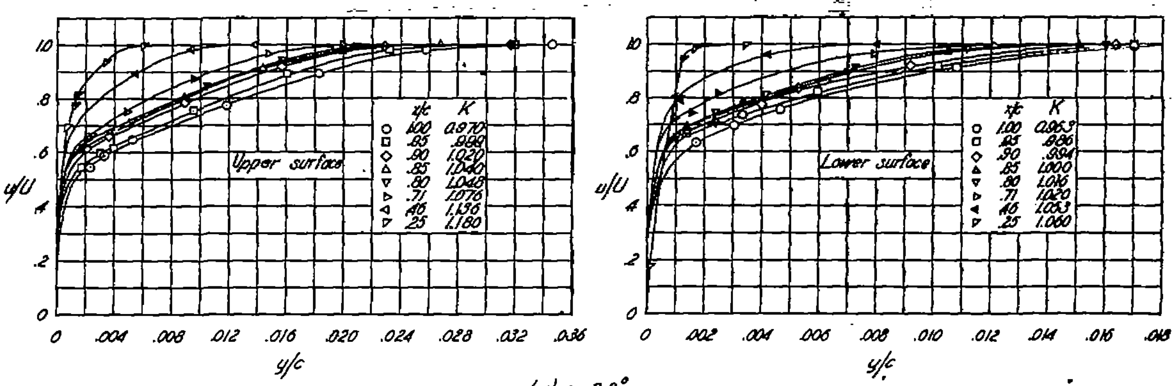

(g) $\alpha_0 = 2.0°$

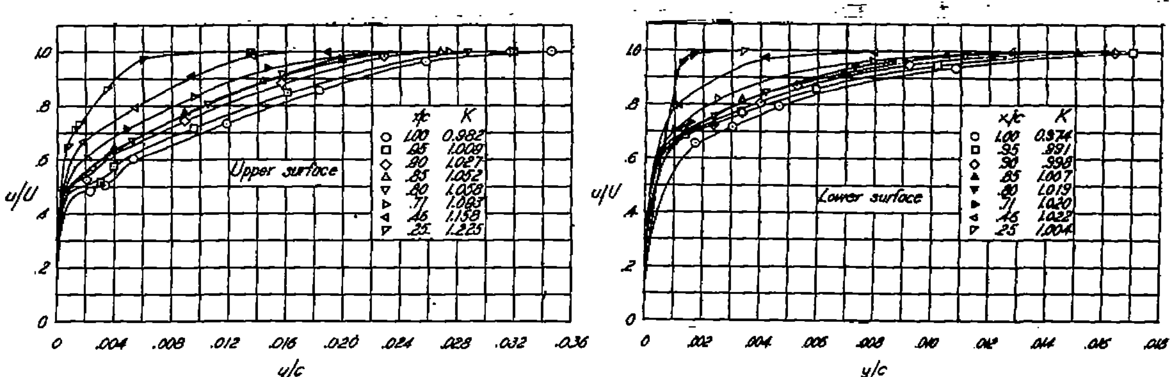

(h) $\alpha_0 = 4.1°$

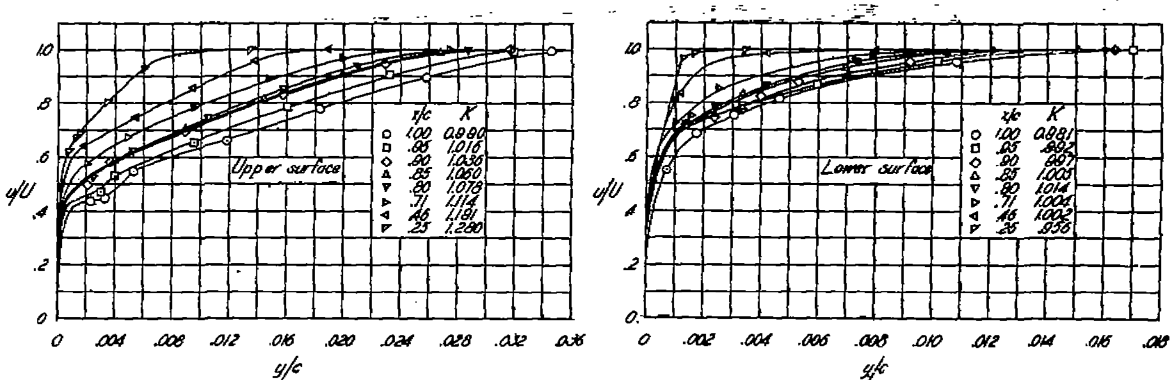

(i) $\alpha_0 = 6.1°$

Figure 2. - Continued.

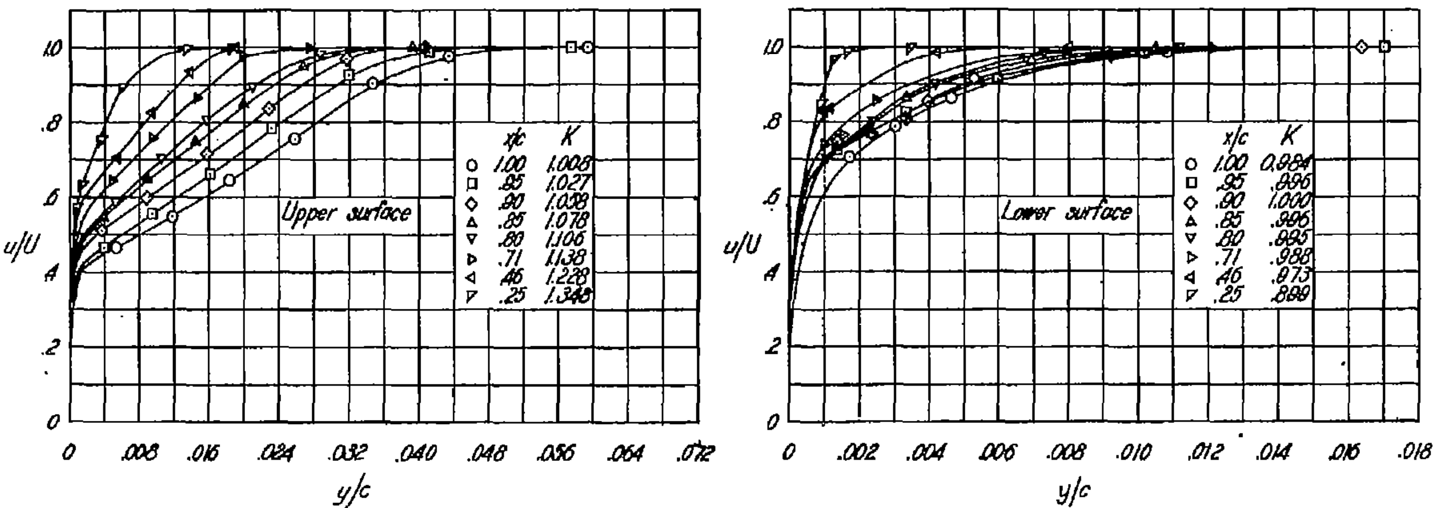

(j) $\alpha_0 = 8.2^\circ$

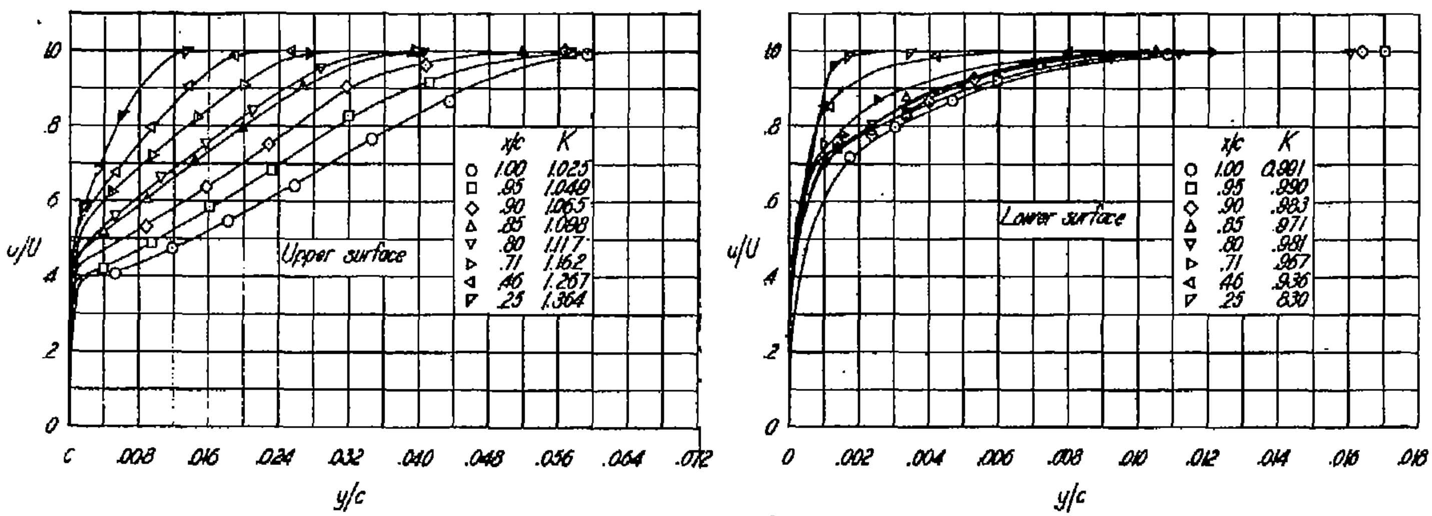

(k) $\alpha_0 = 10.2^\circ$

Figure 2 -Concluded.

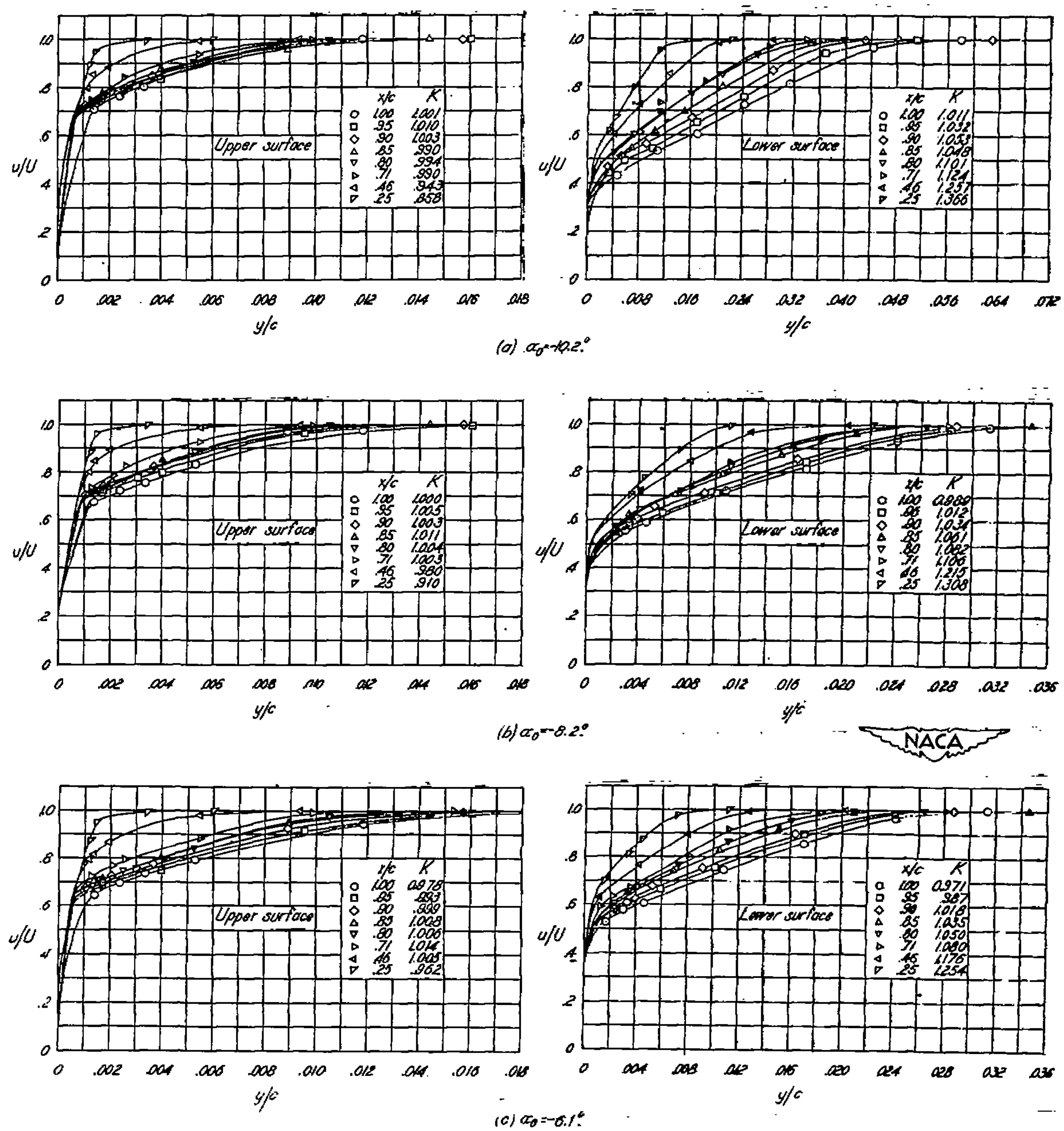

Figure 3.- Boundary-layer velocity profiles on NACA 0009 airfoil with 0.25c plain flap. δ_f=0°.

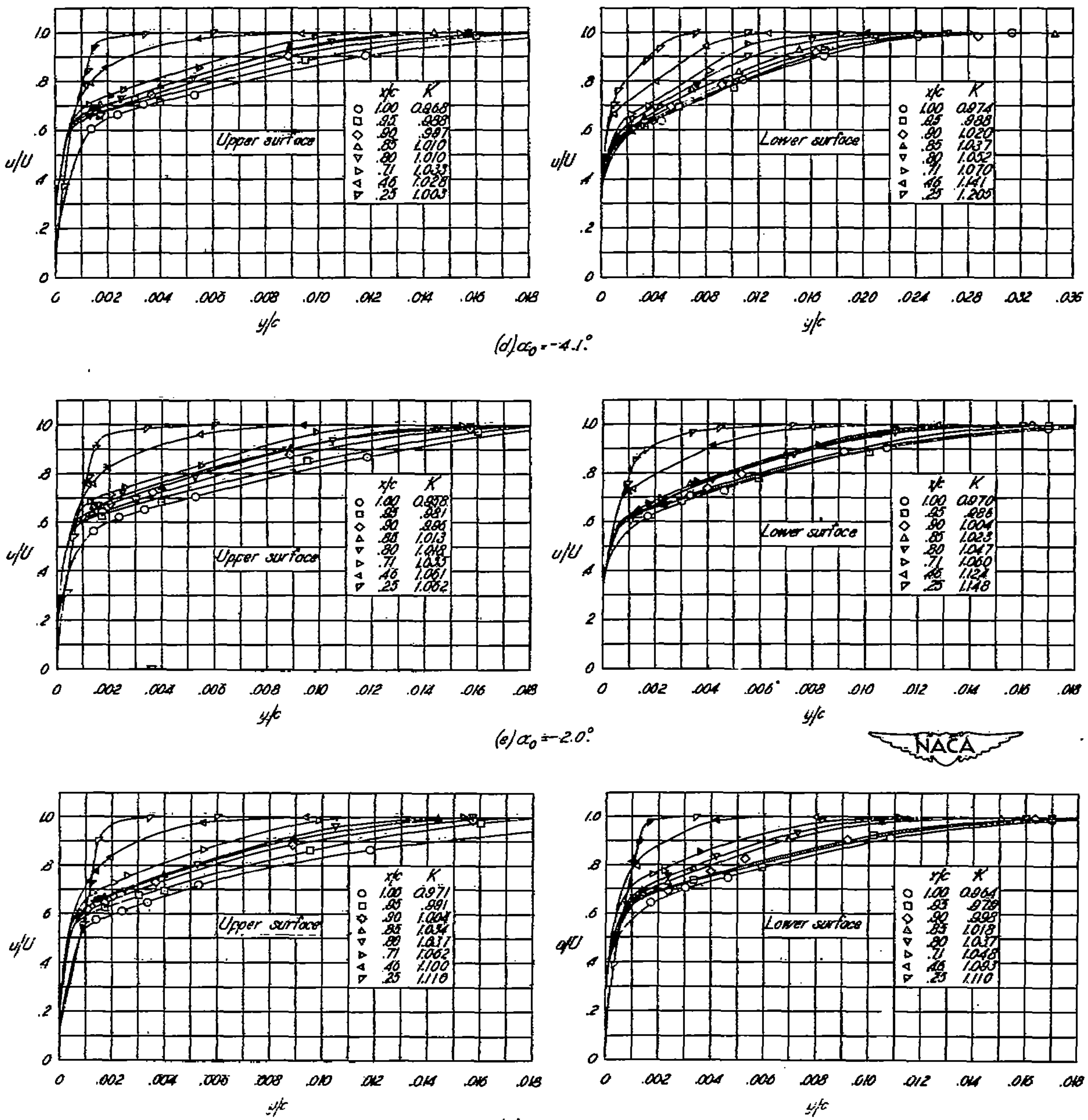

(d) $\alpha_0 = -4.1°$

(e) $\alpha_0 = -2.0°$

(f) $\alpha_0 = 0°$

Figure 3.- Continued.

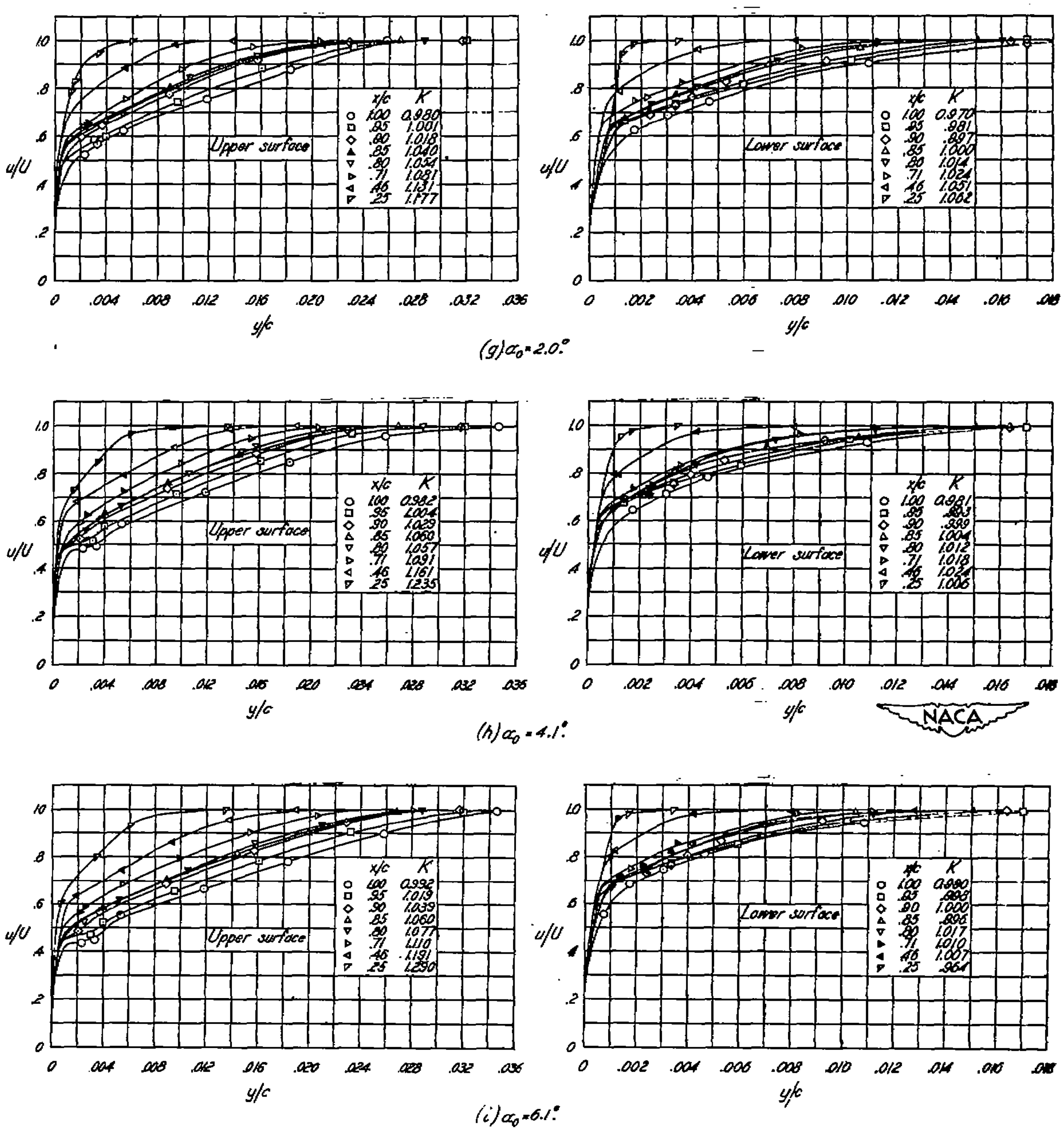

Figure 3.— Continued.

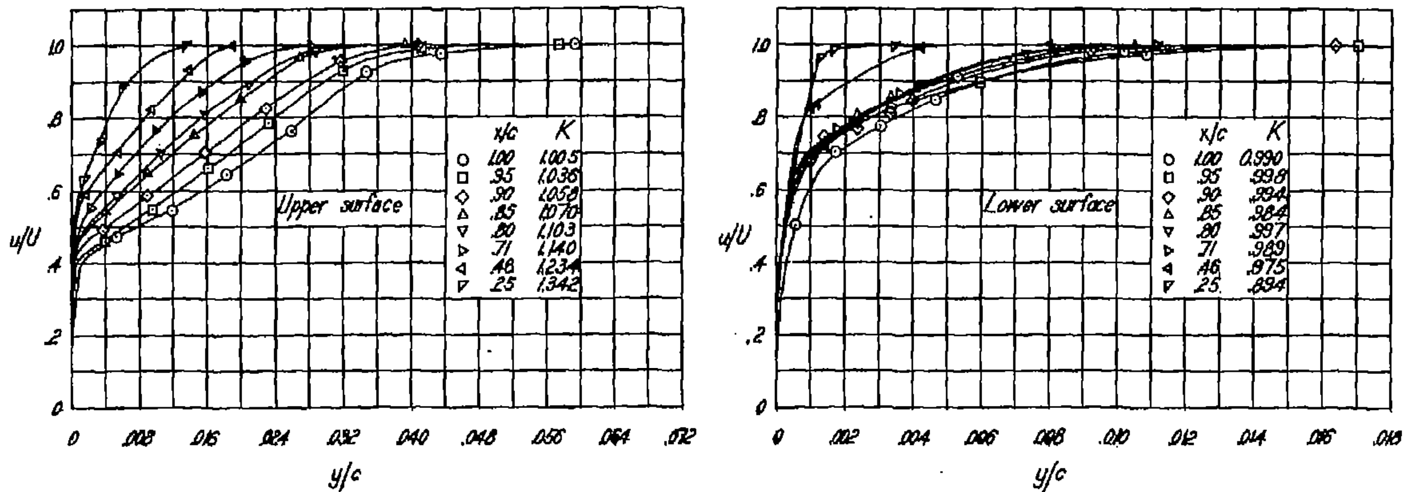

(j) $\alpha_0 = 8.2^\circ$.

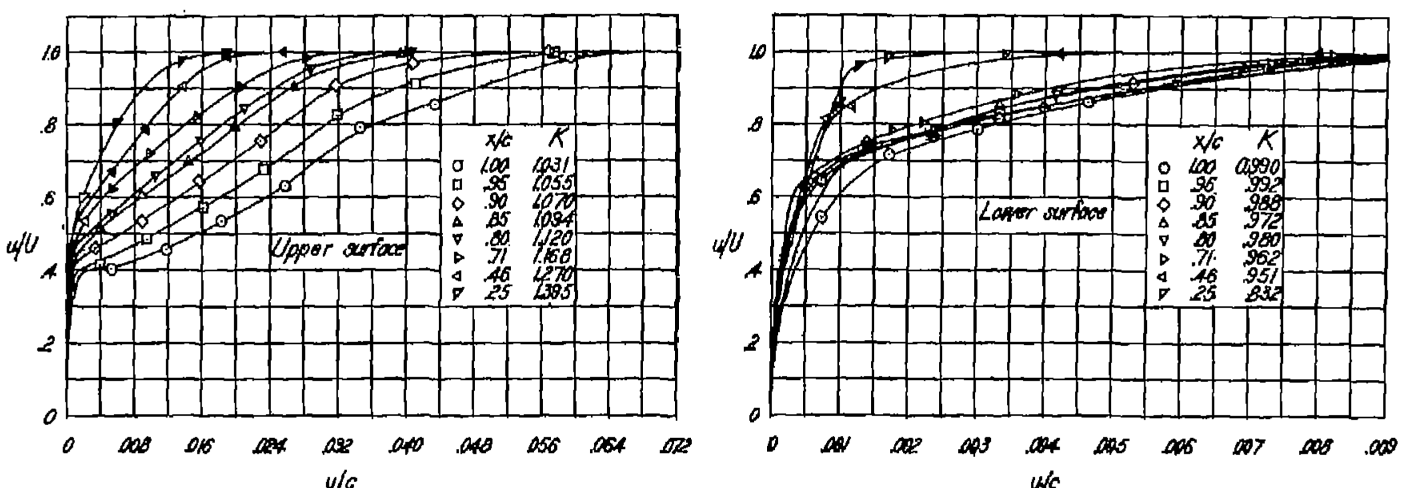

(k) $\alpha_0 = 10.2^\circ$.

Figure 9.- Concluded.

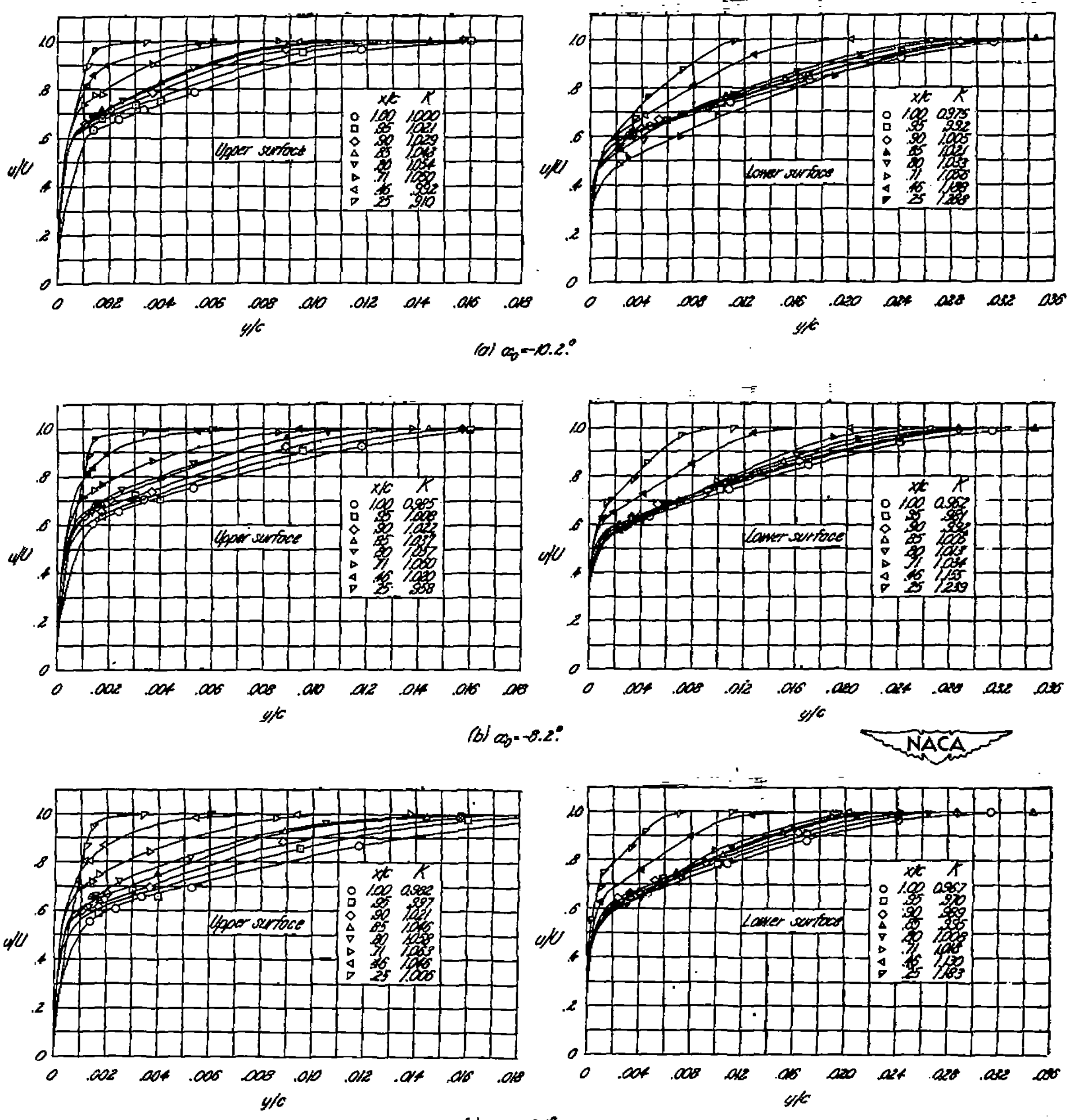

Figure 4.- Boundary-layer velocity profiles on NACA 0009 airfoil with 0.25c plain flap. δ_f=5°.

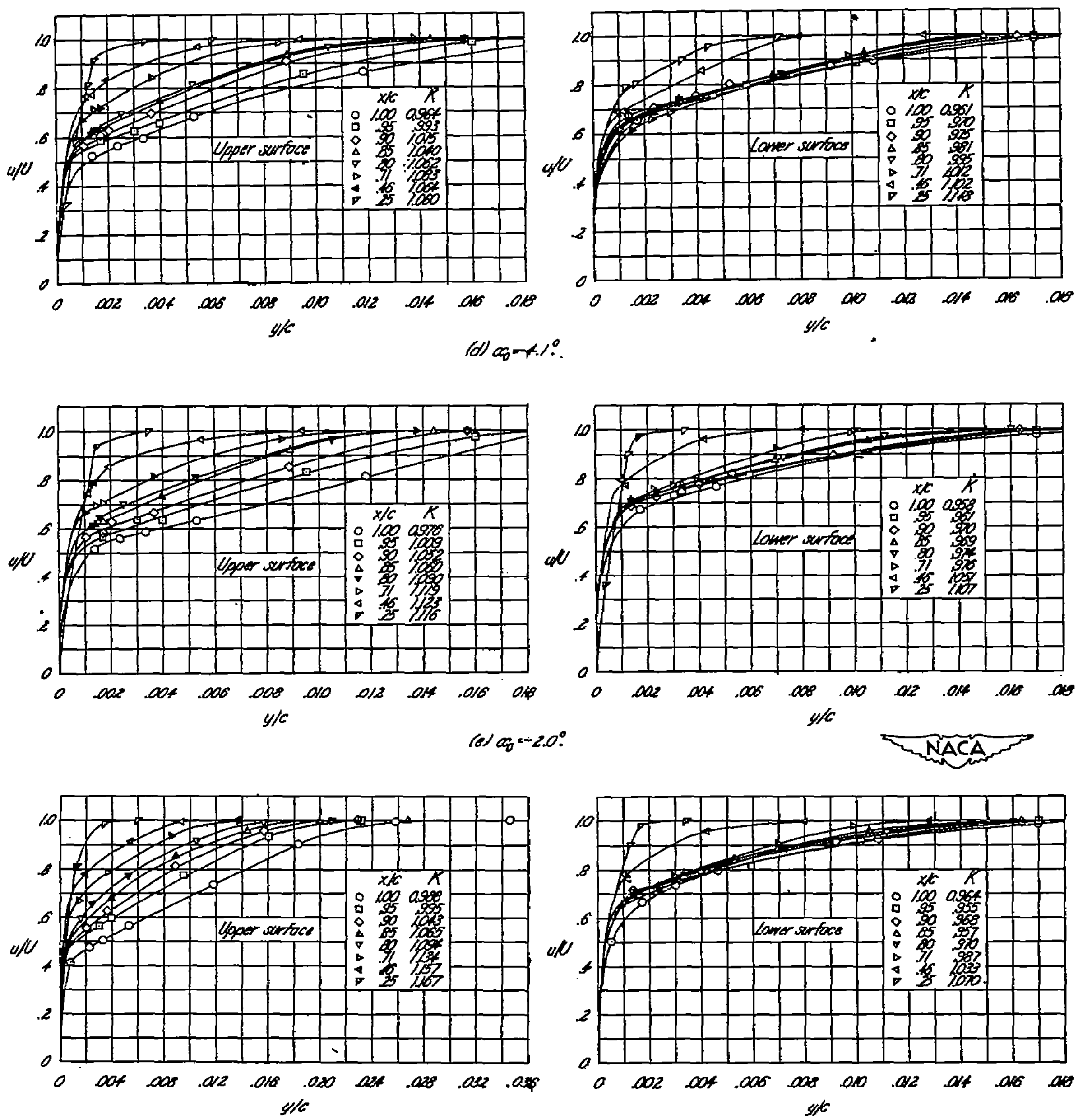

(d) $\alpha_0 = -4.1°$.

(e) $\alpha_0 = -2.0°$.

(f) $\alpha_0 = 0°$.

Figure 4.- Continued.

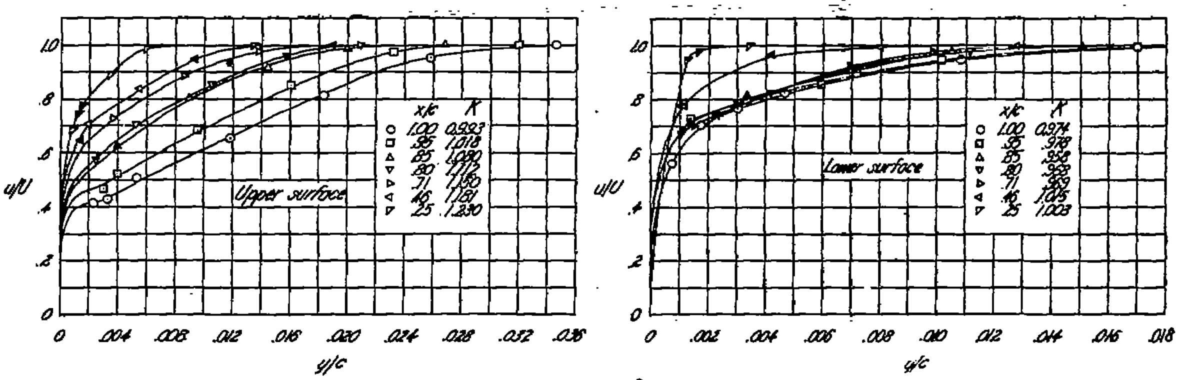

(g) $\alpha_0 = 2.1°$

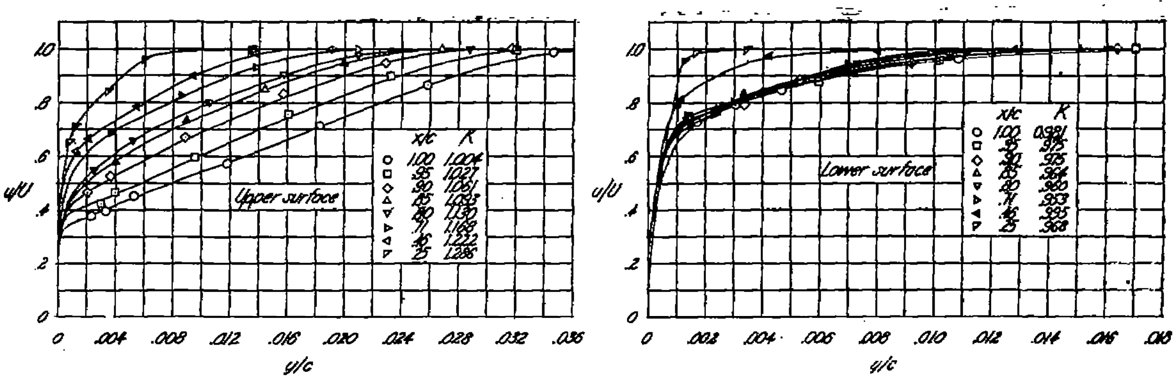

(h) $\alpha_0 = 4.1°$

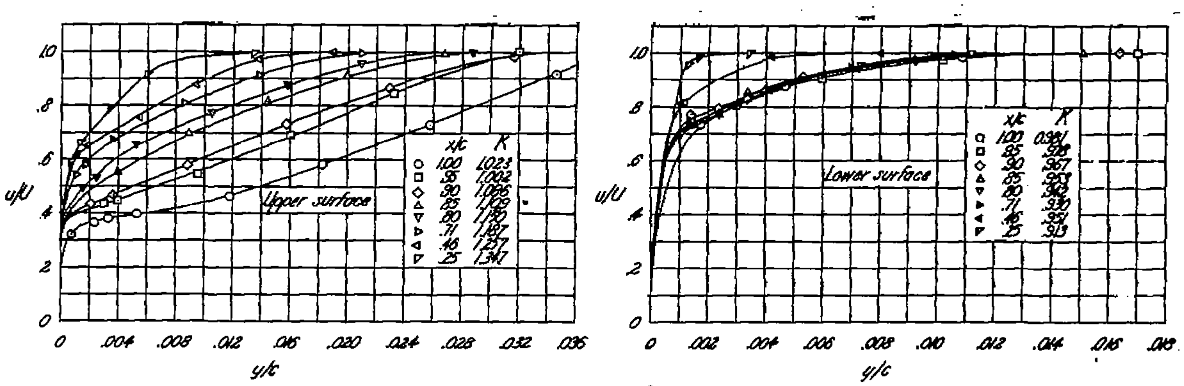

(i) $\alpha_0 = 6.2°$

Figure 4.- Continued.

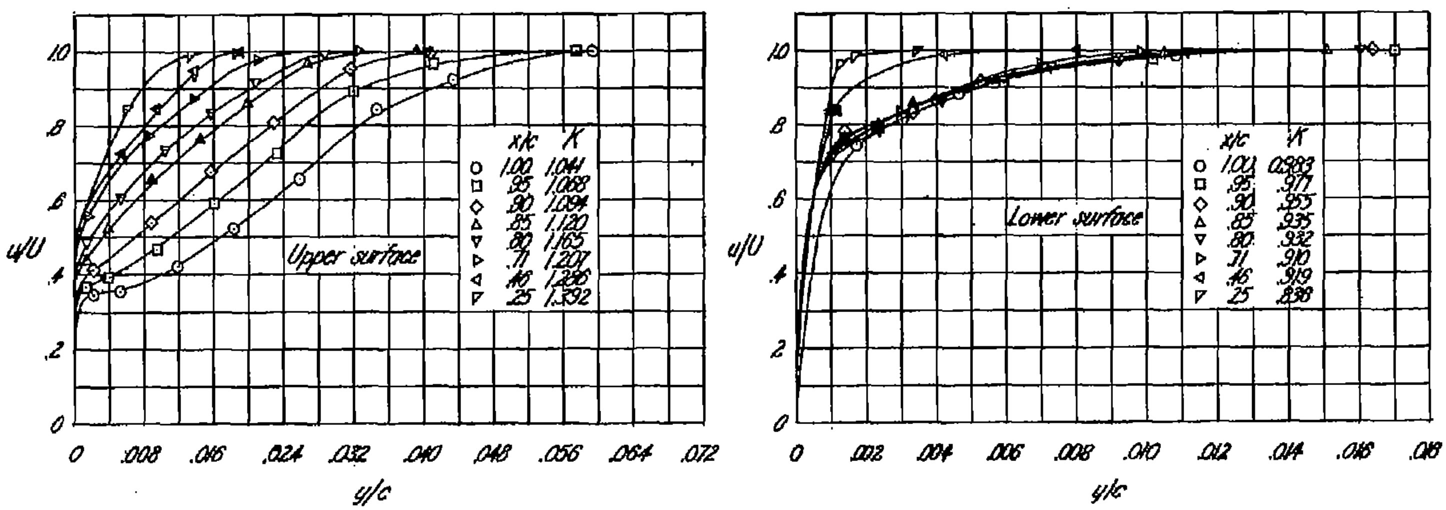

(j) $\alpha_0 = 8.2°$.

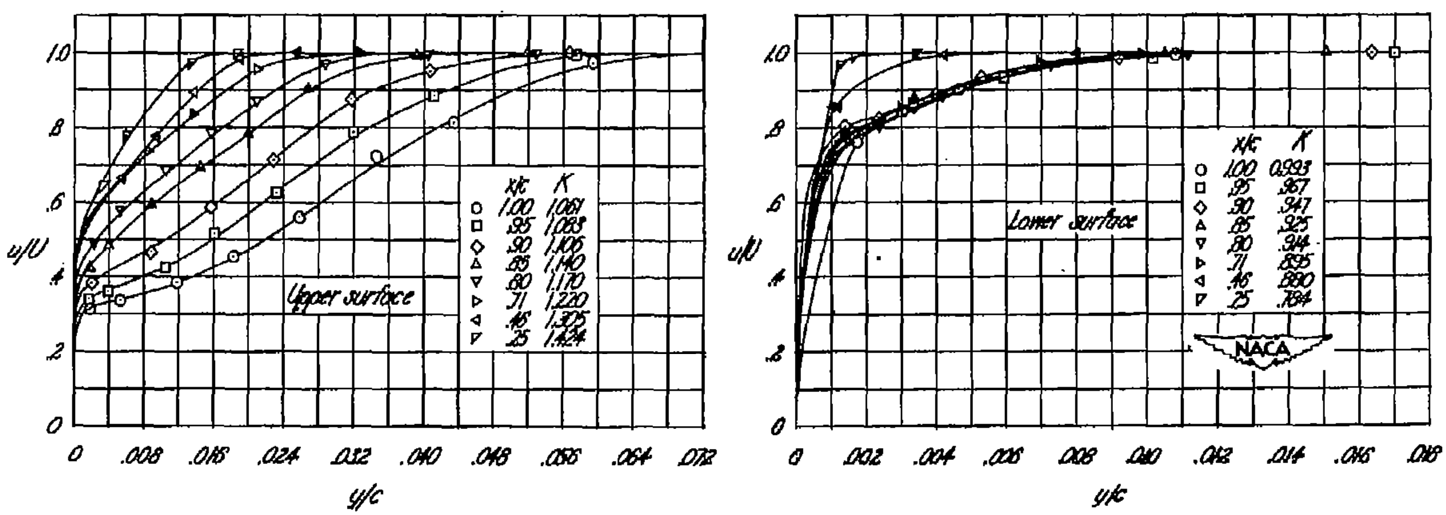

(k) $\alpha_0 = 10.2°$.

Figure 7.- Concluded.

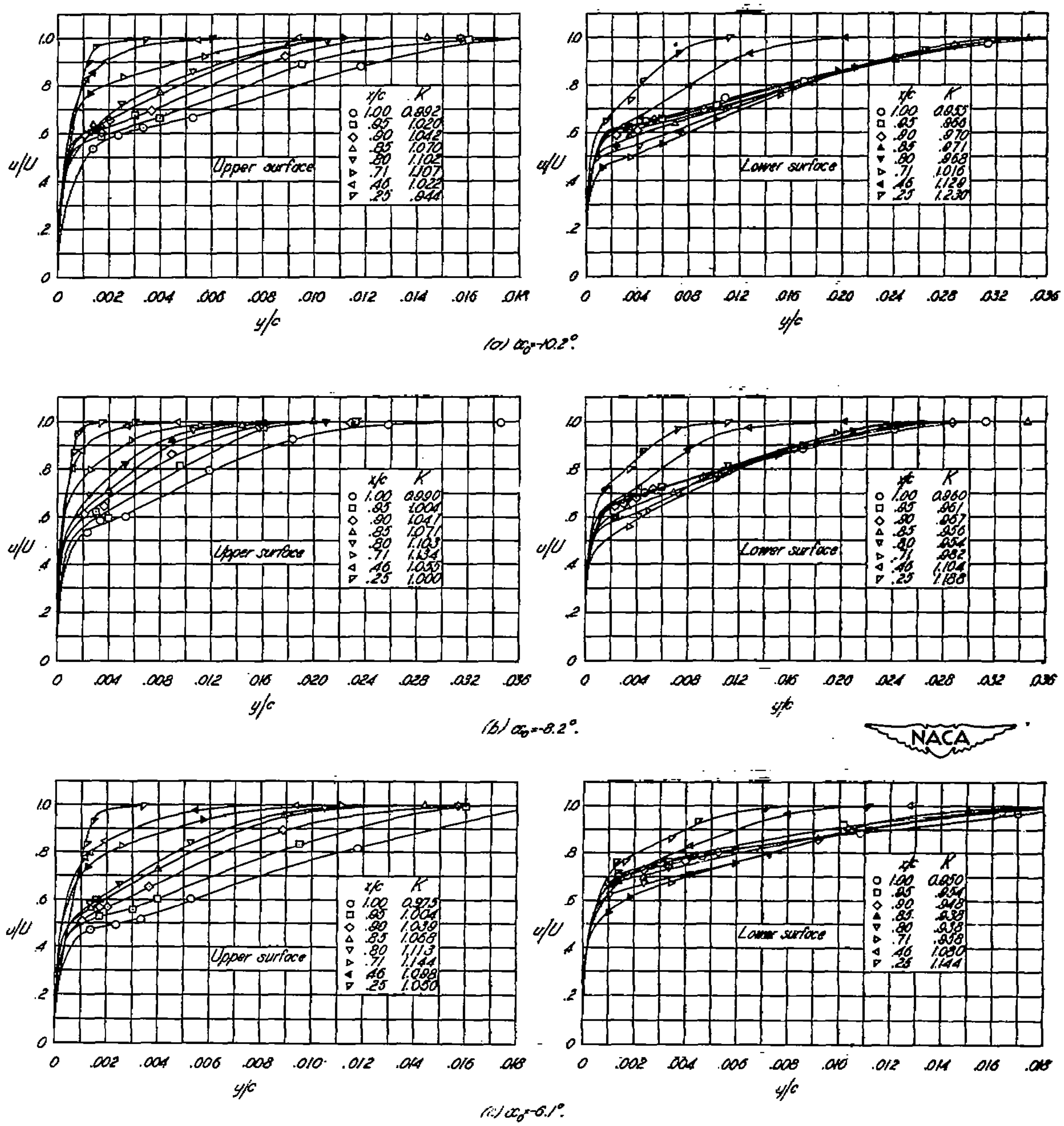

Figure 5.- Boundary-layer velocity profiles on NACA 0009 airfoil with 0.25c plain flap. δ_f=-10°.

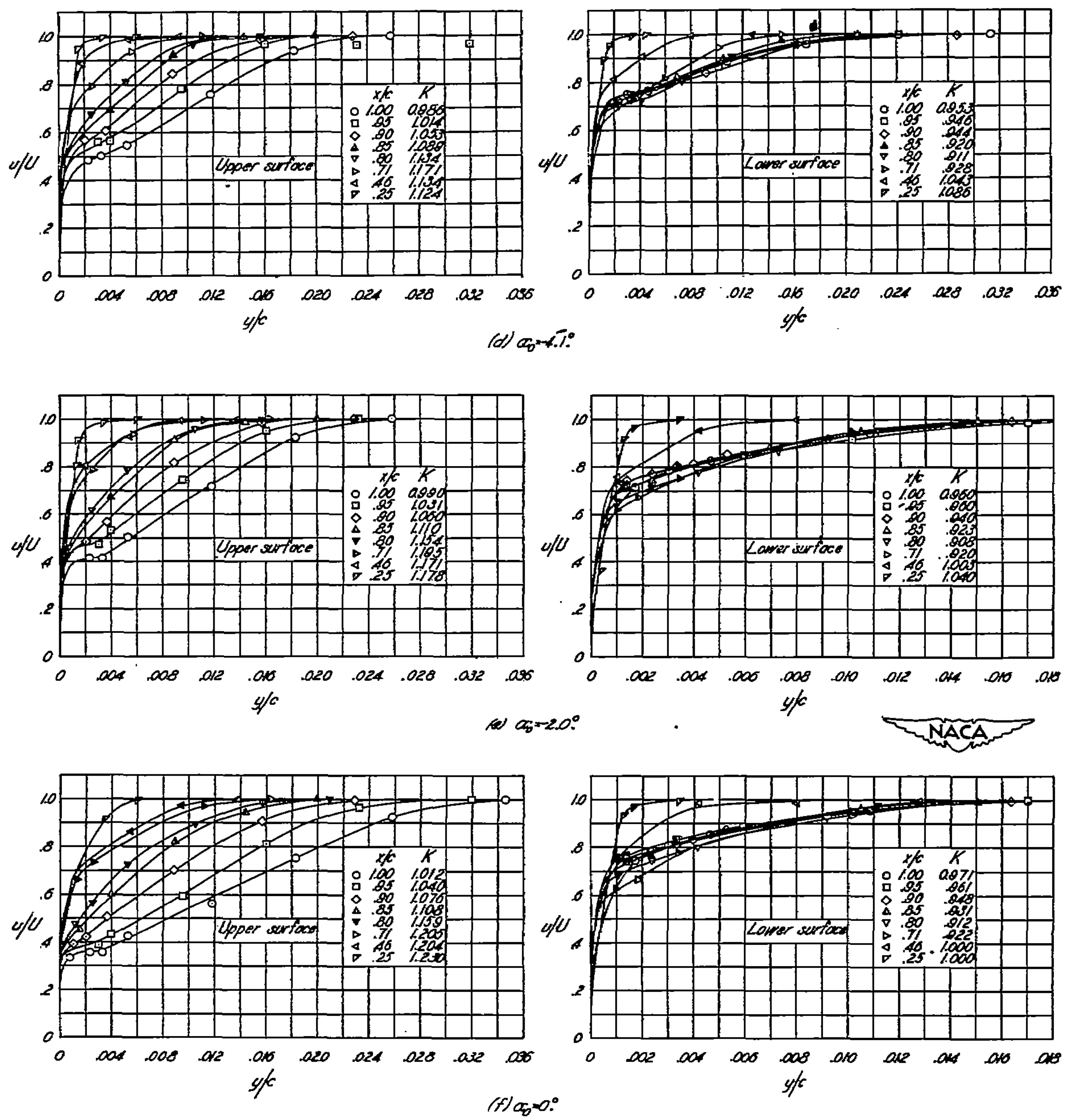

Figure 5.- Continued.

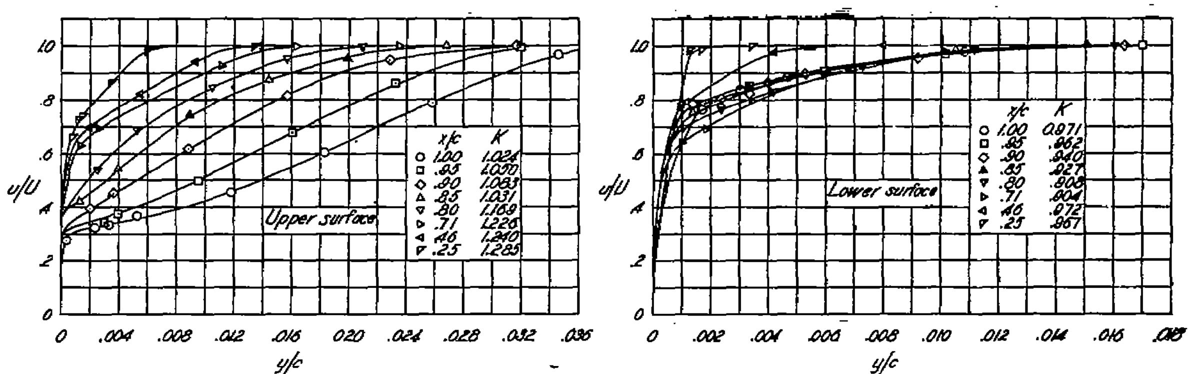

(g) α_0=2.1°.

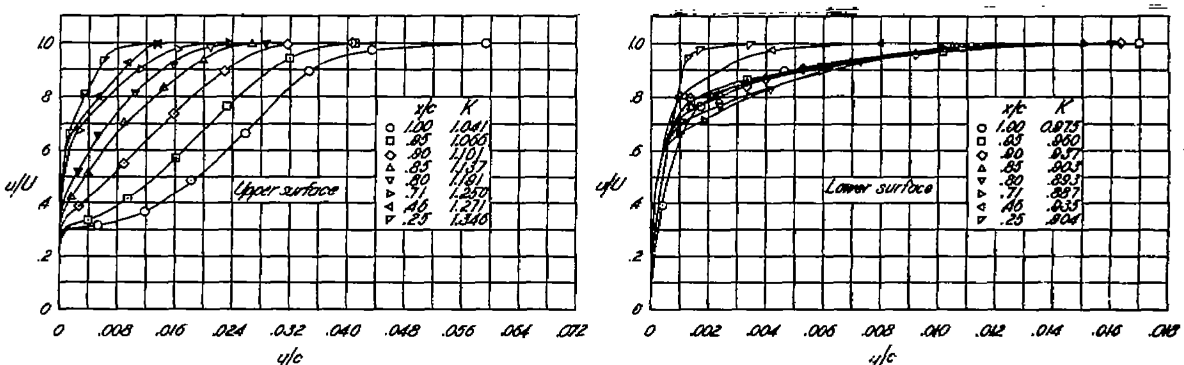

(h) α_0=4.1°.

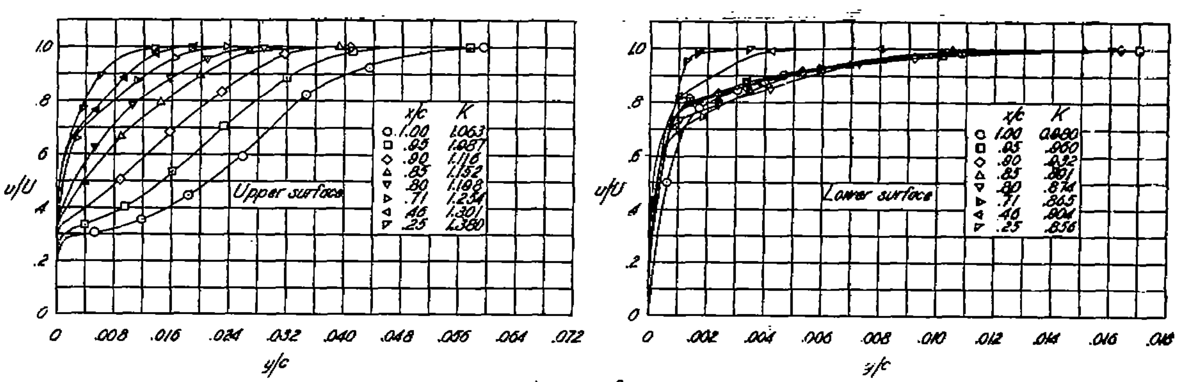

(i) α_0=6.2°.

Figure 5.- Continued.

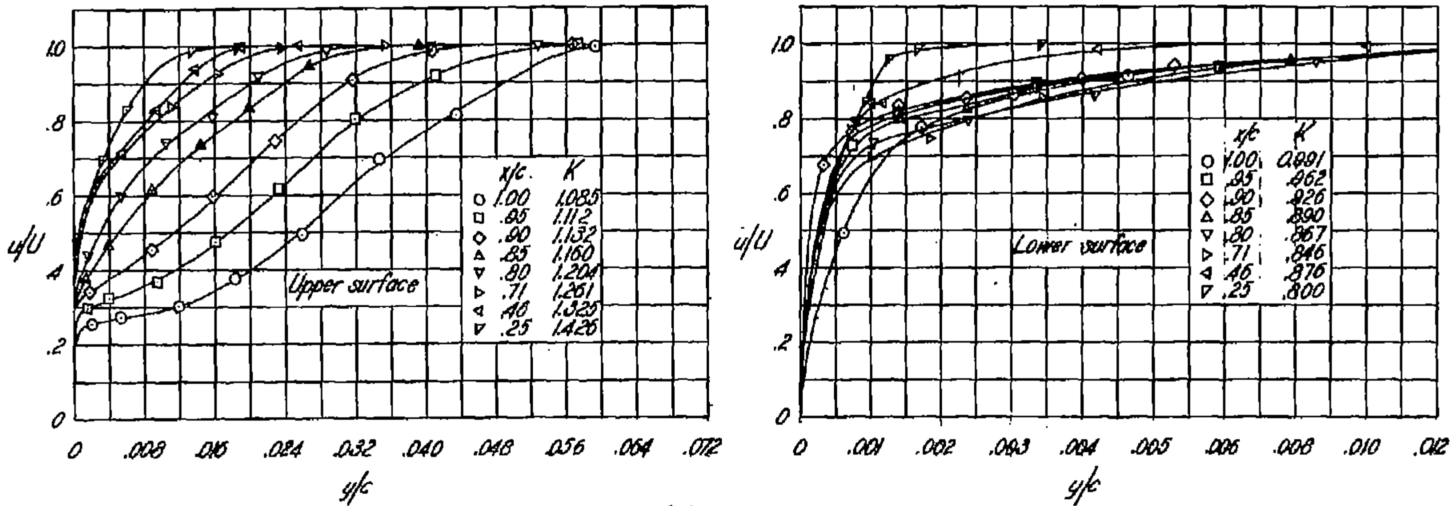

(j) $\alpha_0 = 8.2°$.

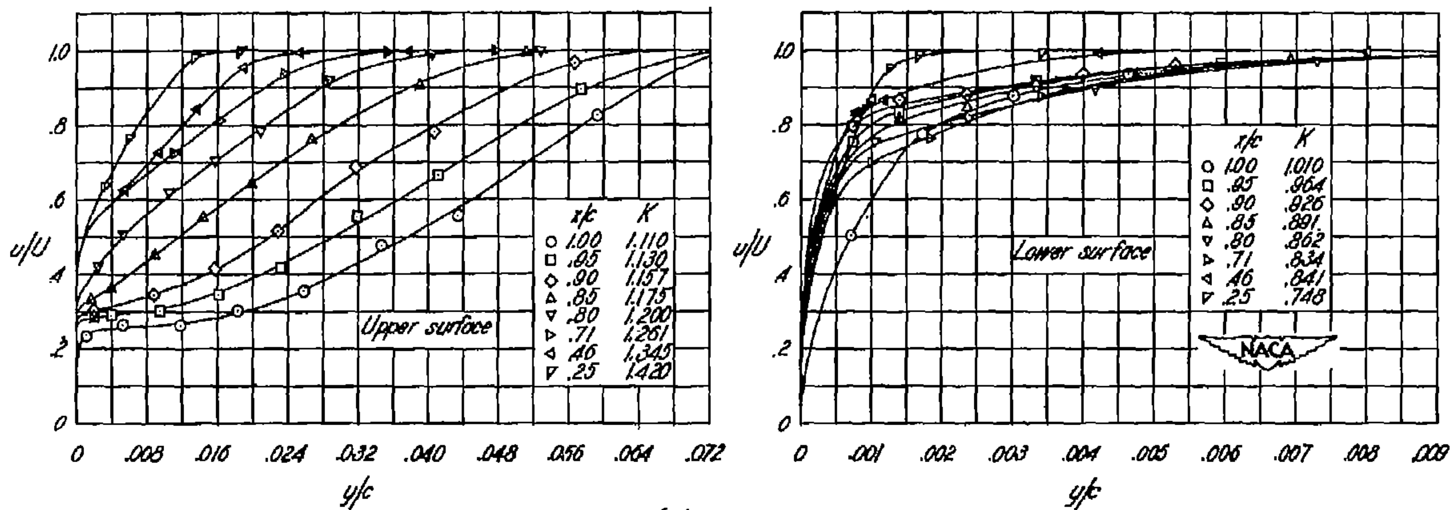

(k) $\alpha_0 = 10.2°$.

Figure 5.- Concluded.

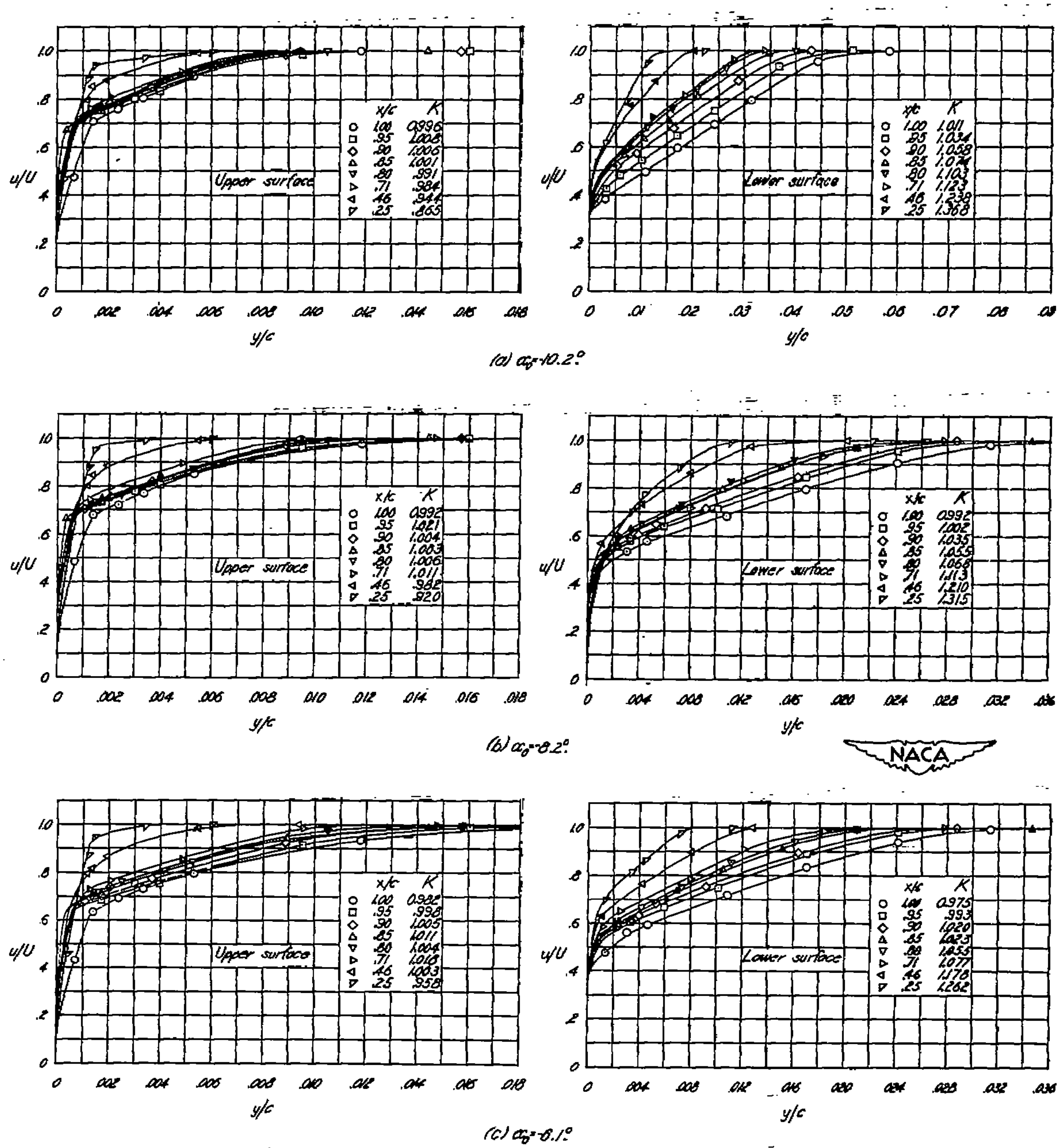

Figure 6.- Boundary-layer velocity profiles on NACA 0009 airfoil with 0.50c plain flap. δ_f=0°.

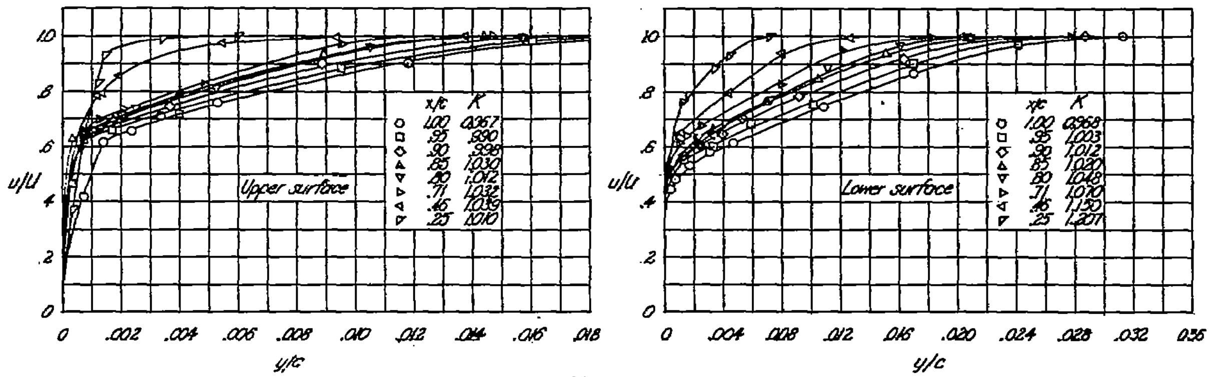

(d) $\alpha_0 = -4.1°$

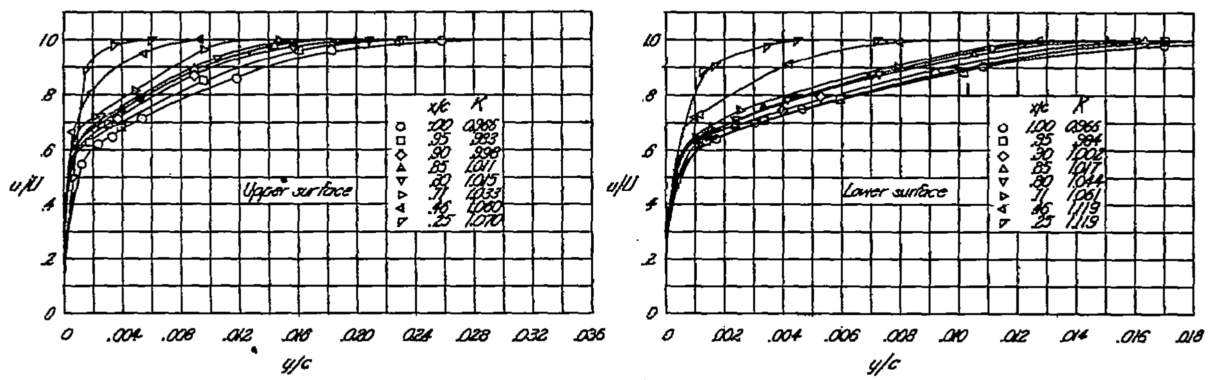

(e) $\alpha_0 = -2.0°$

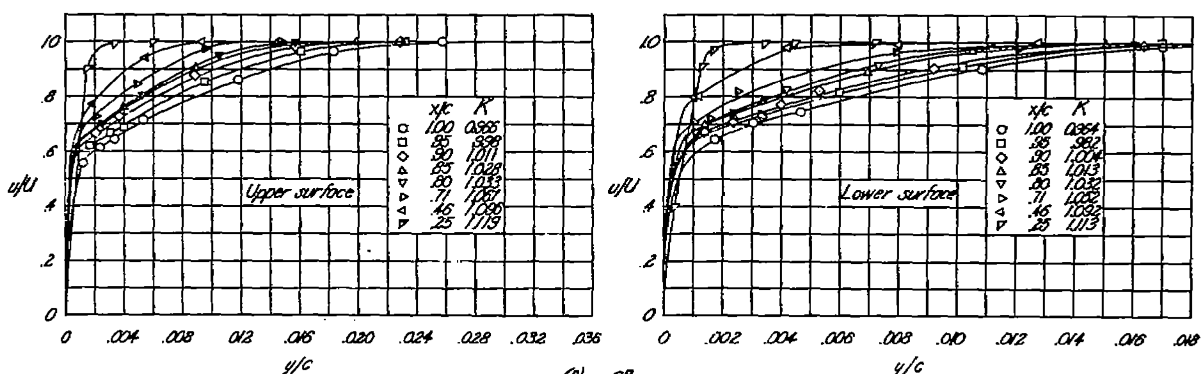

(f) $\alpha_0 = 0°$

Figure 6.- Continued.

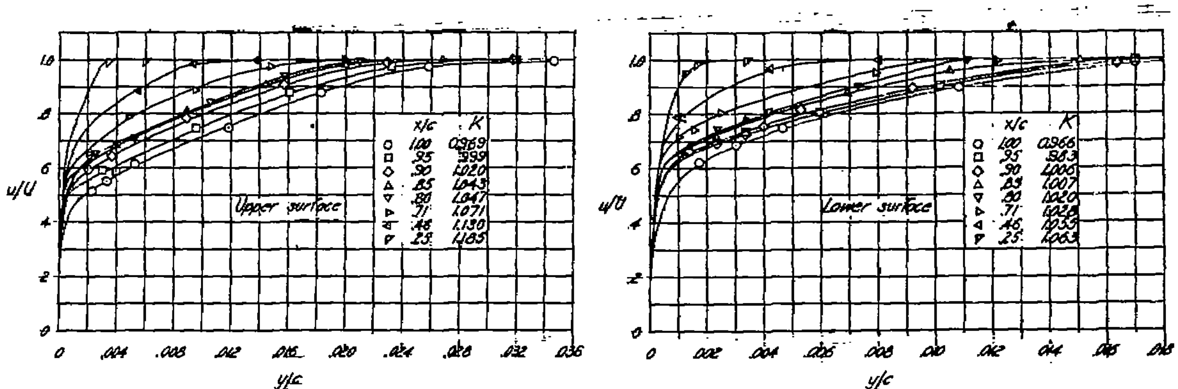

(g) $\alpha_0 = 2.0°$

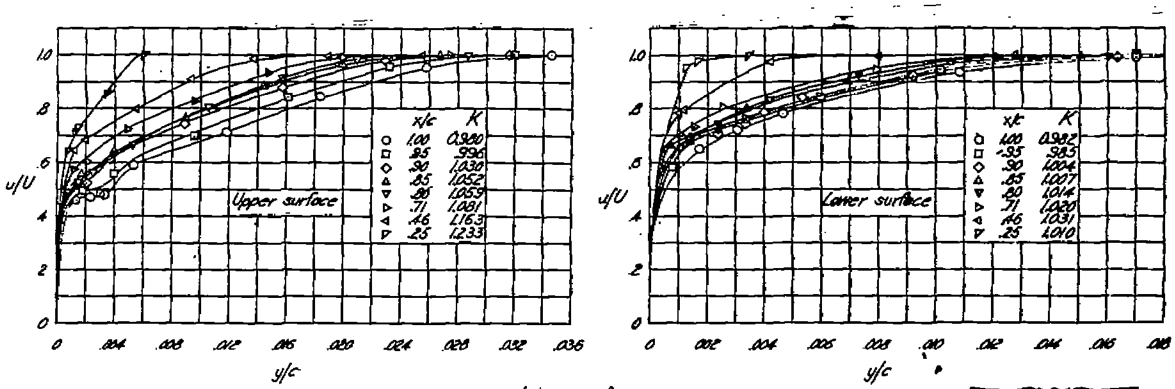

(h) $\alpha_0 = 4.1°$

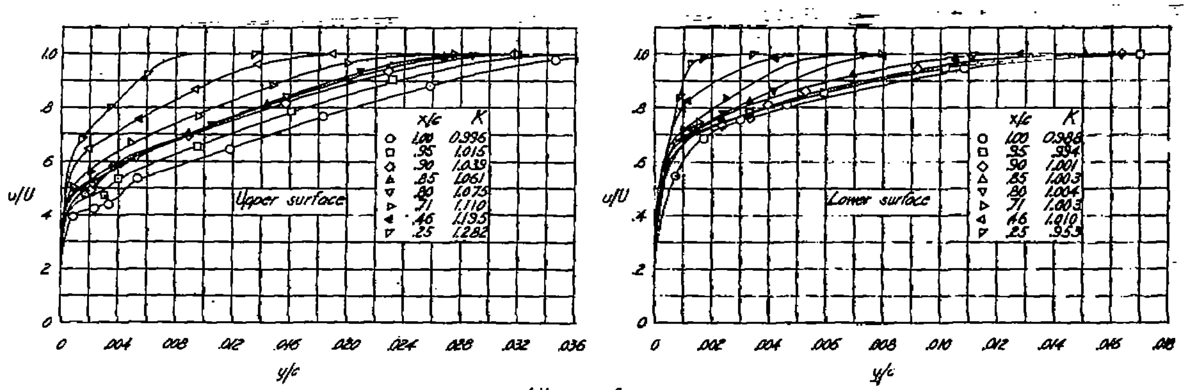

(i) $\alpha_0 = 6.1°$

Figure 6. - Continued.

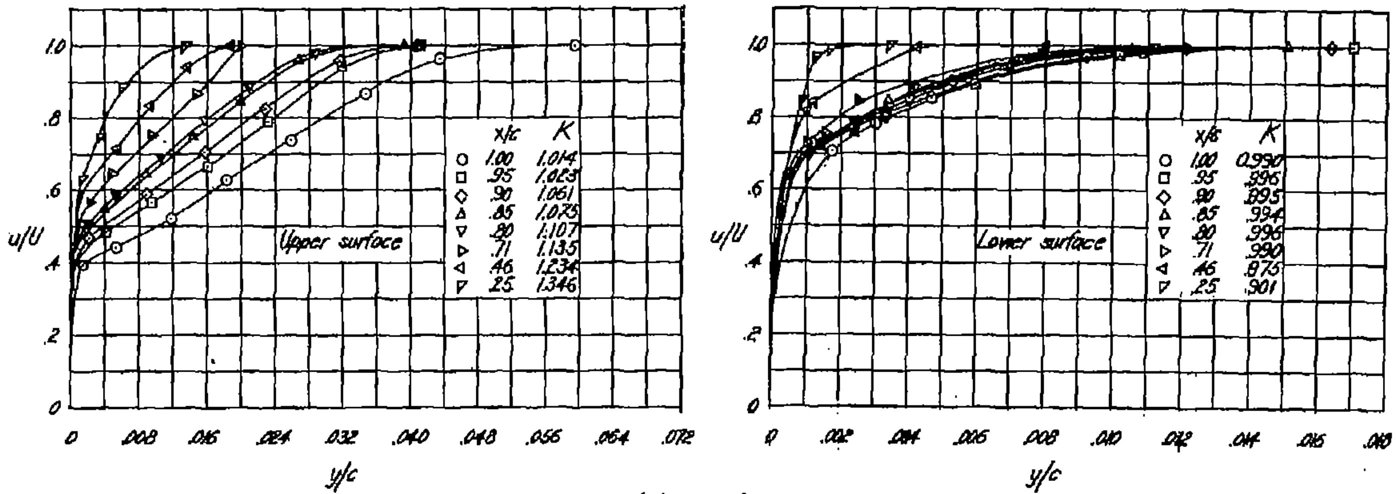

(j) $\alpha_0 = 8.2°$

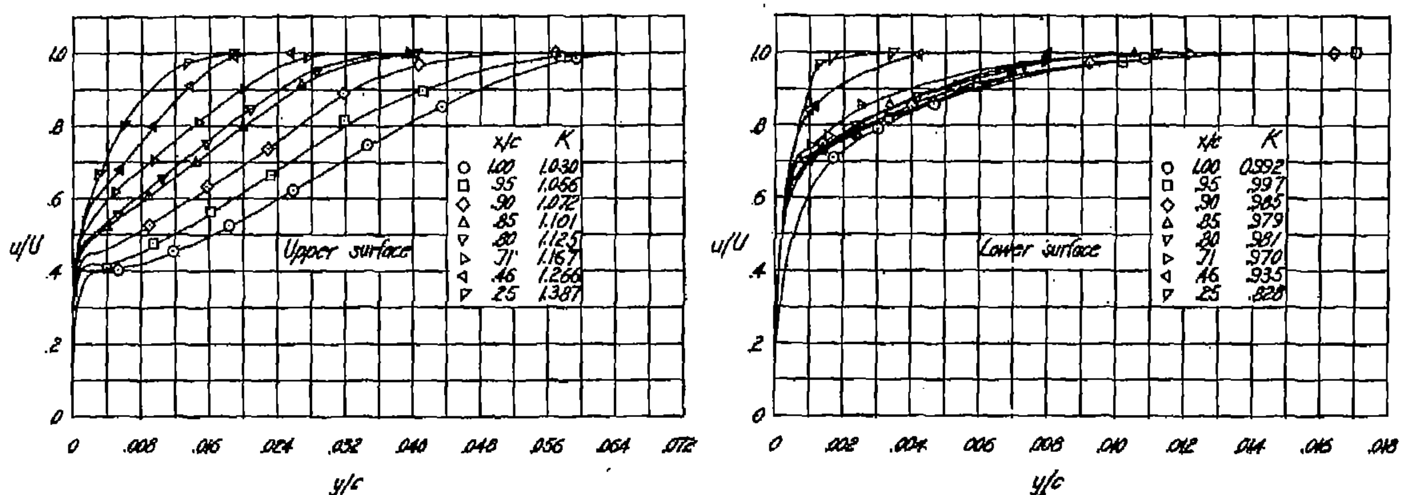

(k) $\alpha_0 = 10.2°$

Figure 6.- Concluded.

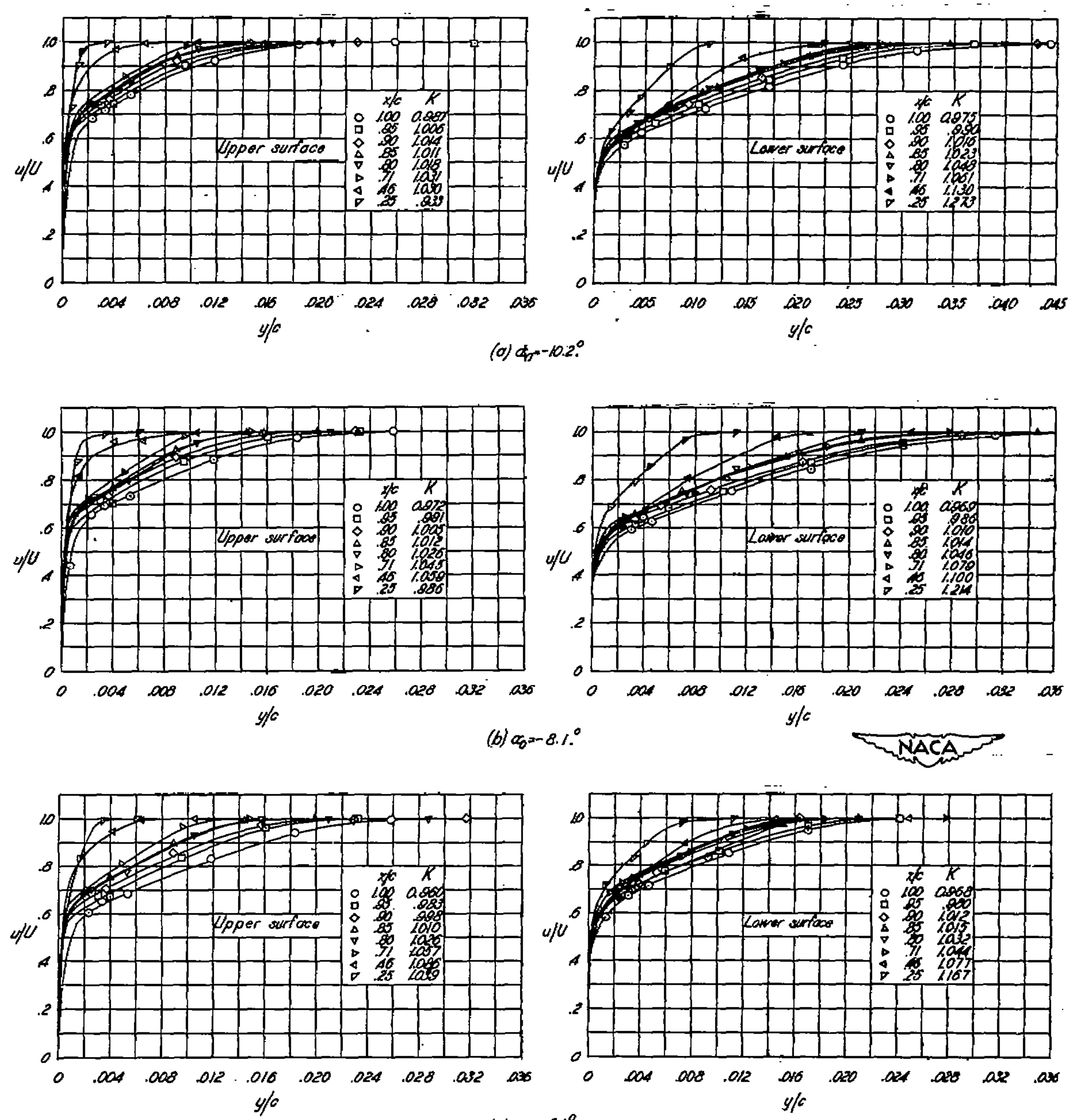

Figure 7.- Boundary-layer velocity profiles on NACA 0009 airfoil with 0.50c plain flap. δ_f = 5°.

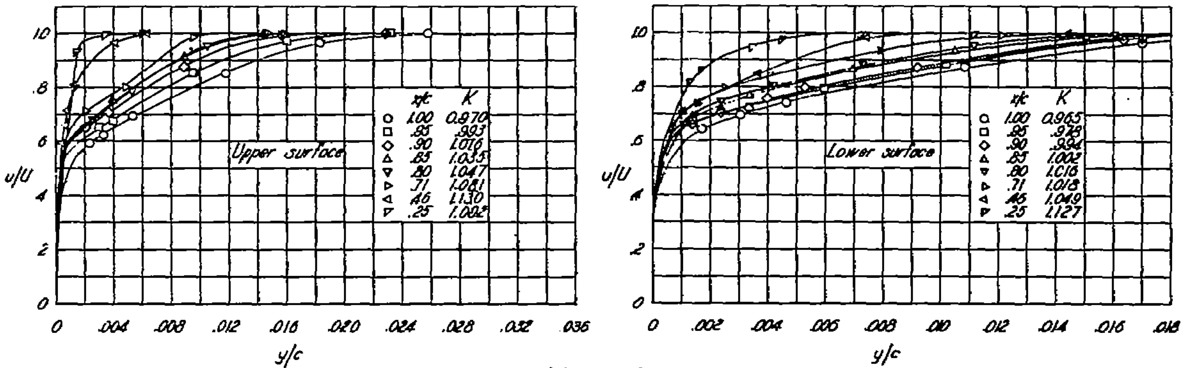

(d) $\alpha_0 = -4.0°$

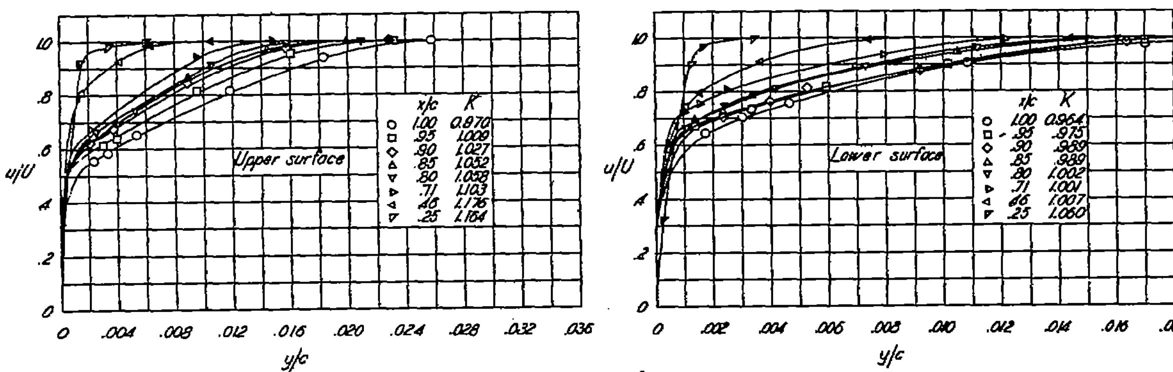

(e) $\alpha_0 = -2.0°$

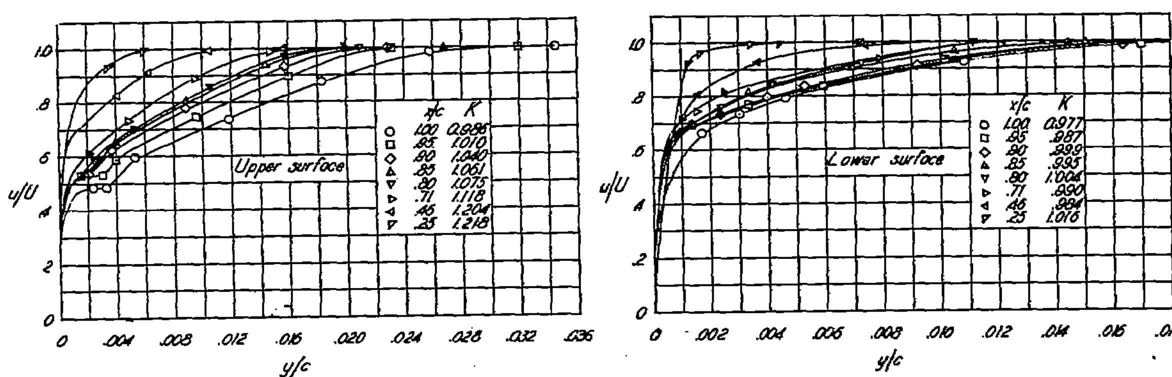

(f) $\alpha_0 = 0.1°$

Figure 7.- Continued.

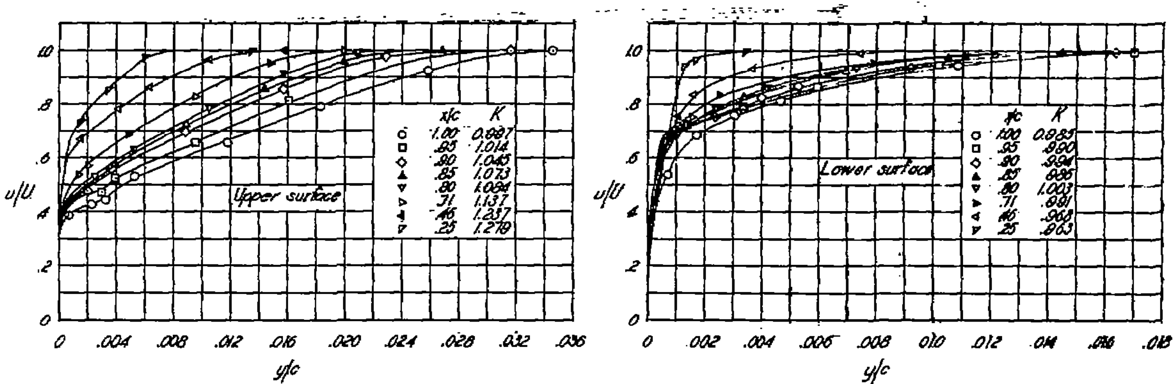

(g) $\alpha_0 = 2.1°$

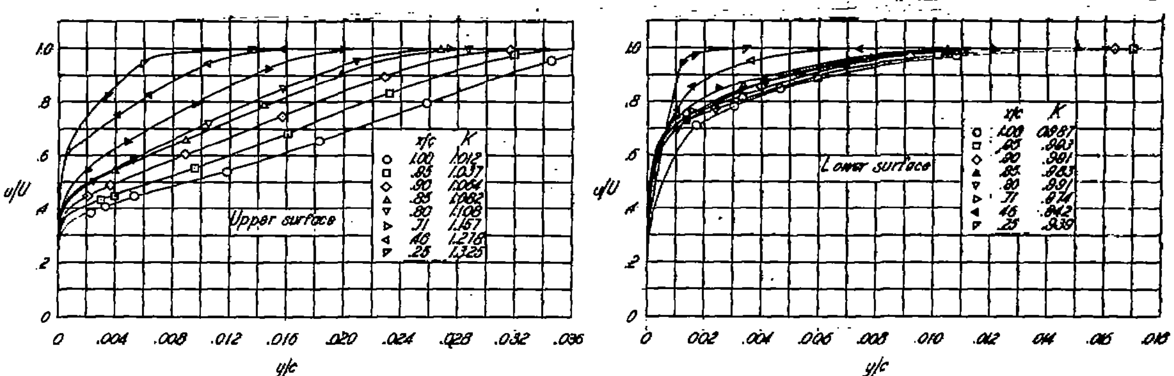

(h) $\alpha_0 = 4.1°$

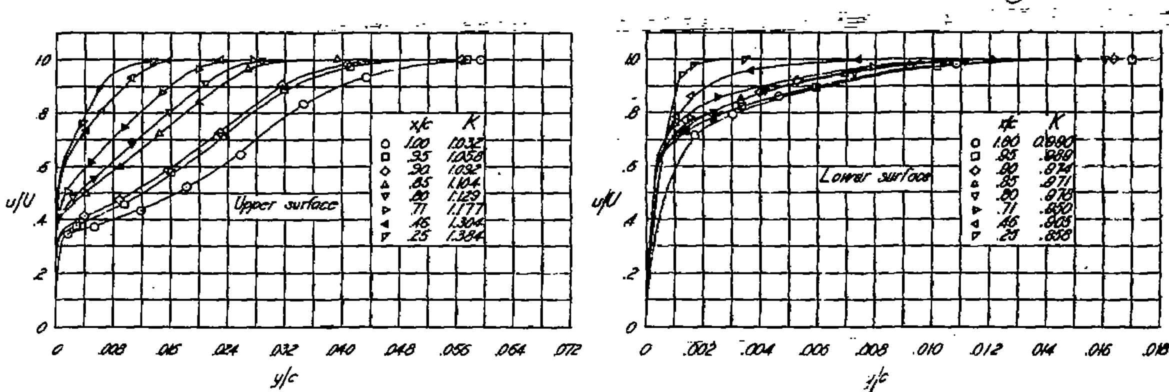

(i) $\alpha_0 = 6.2°$

Figure 7.- Continued.

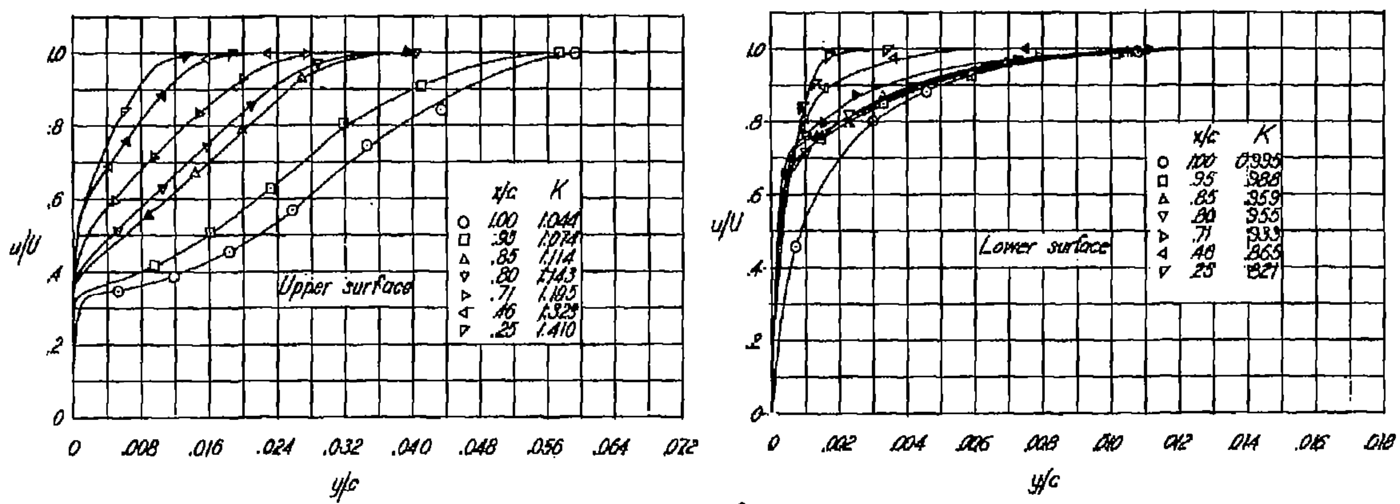

(j) $\alpha_0 = 8.2°$

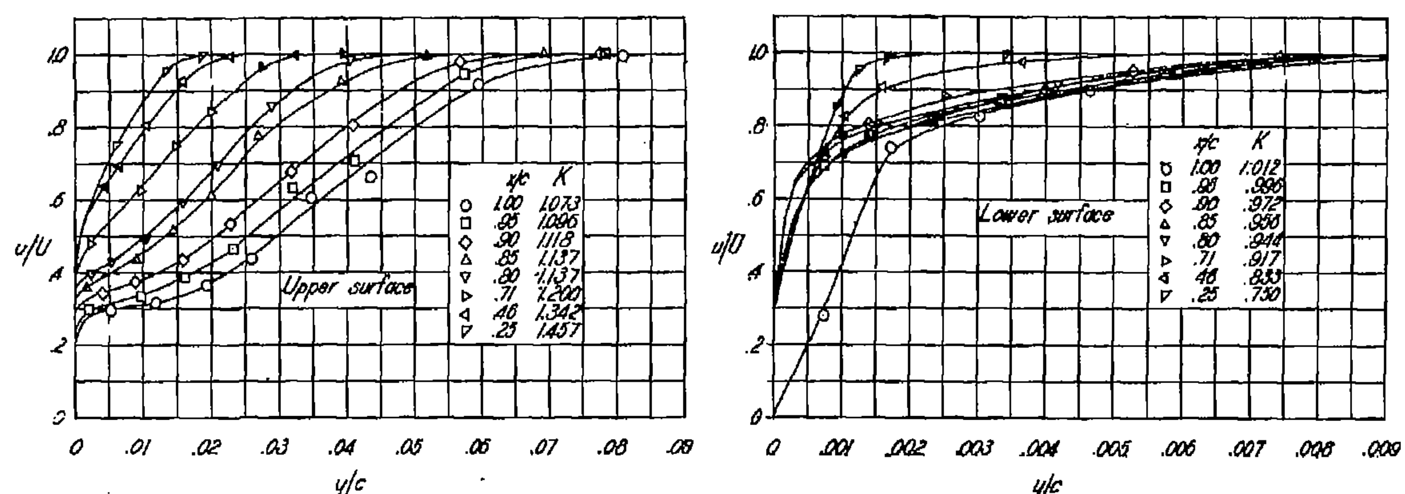

(k) $\alpha_0 = 10.3°$

Figure 7.- Concluded.

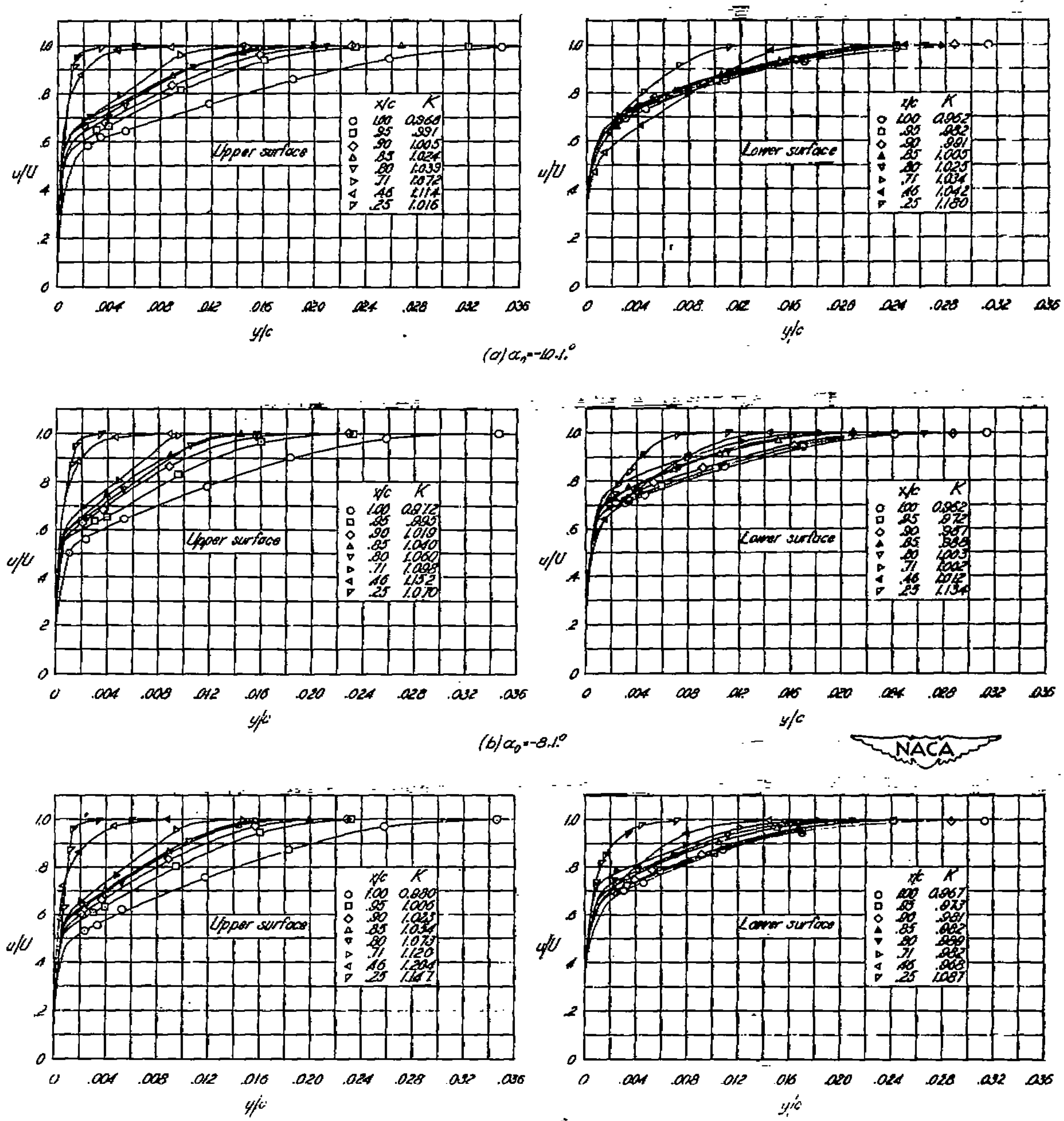

Figure 8.- Boundary-layer velocity profiles on NACA 0009 airfoil with 0.50c plain flap. $\delta_f = 10^\circ$.

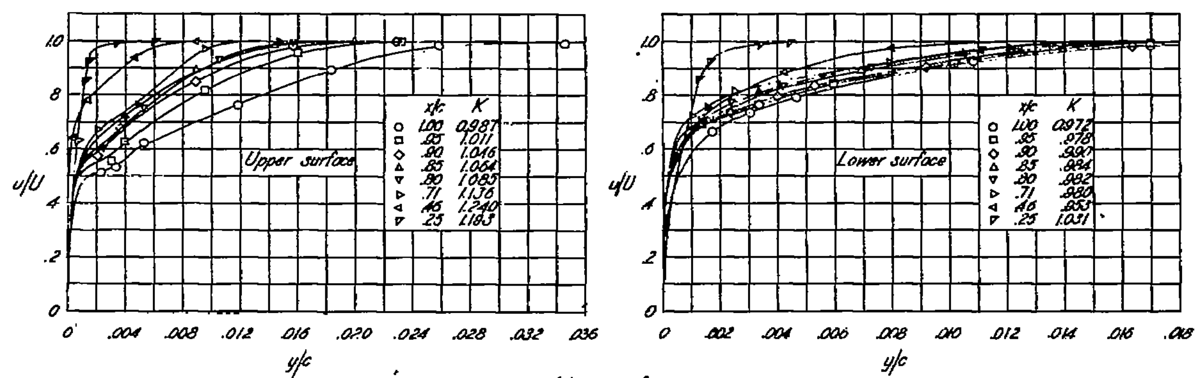

(d) $\alpha_0 = -4.0°$

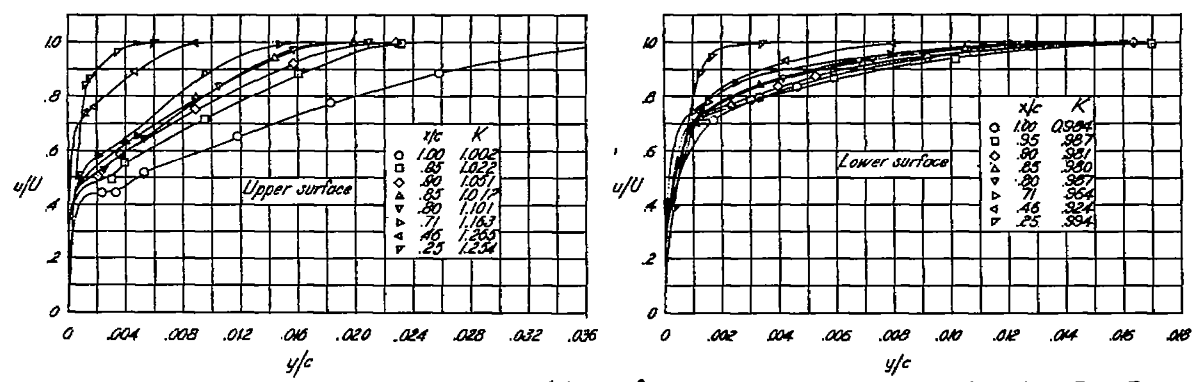

(e) $\alpha_0 = -1.9°$

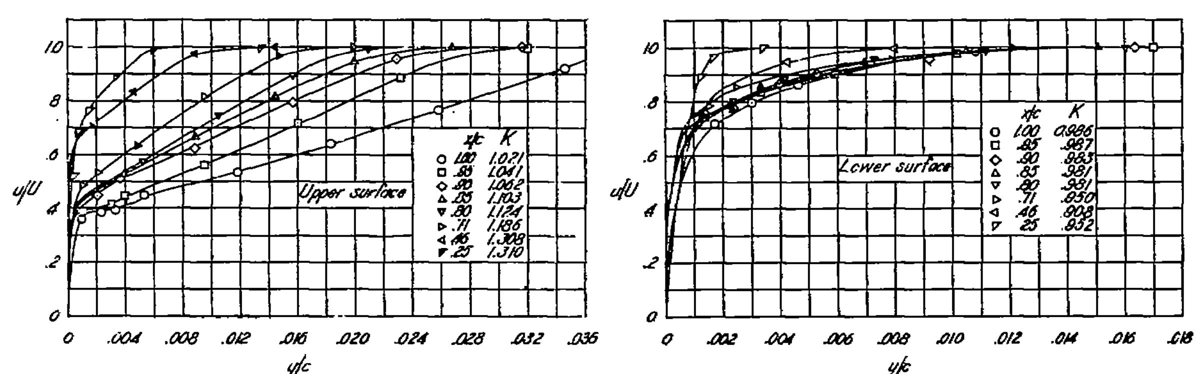

(f) $\alpha_0 = 0.1°$

Figure 8.- Continued.

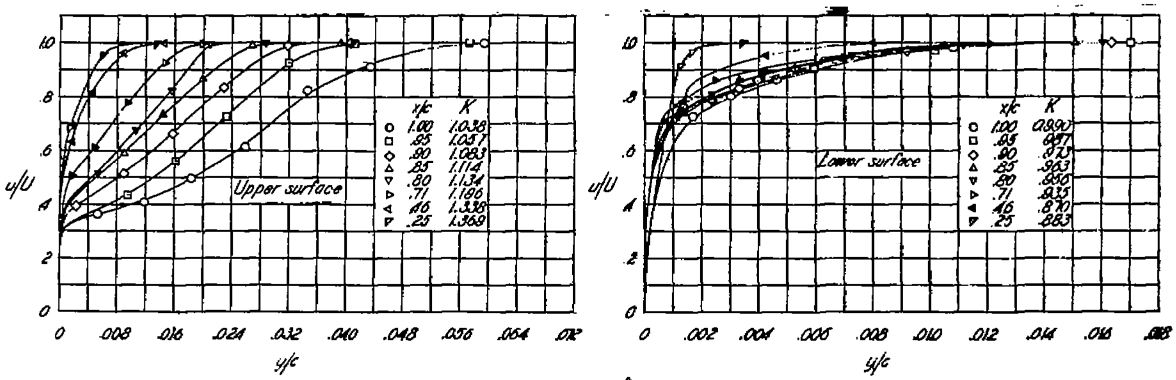

(g) $\alpha_0 = 2.2°$

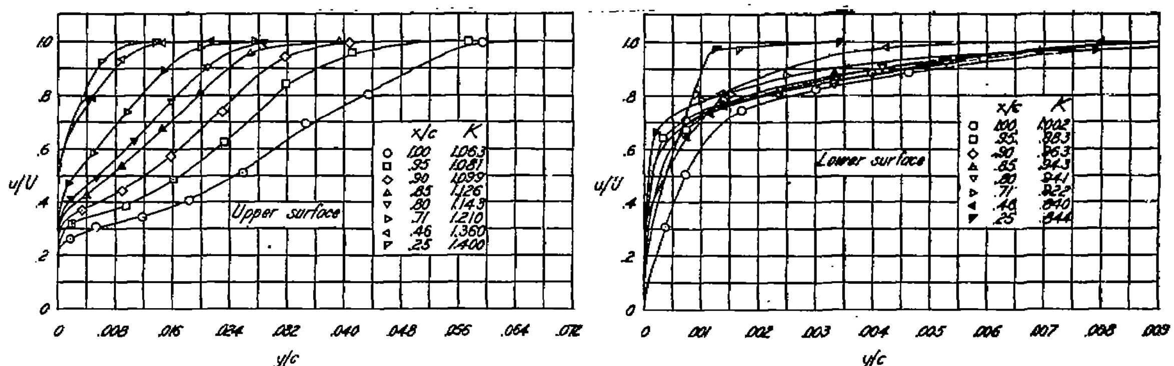

(h) $\alpha_0 = 4.2°$

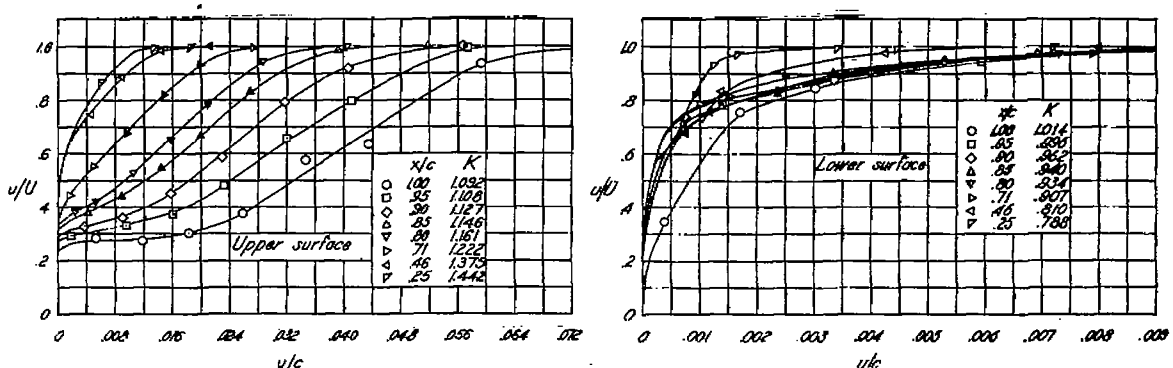

(i) $\alpha_0 = 6.2°$

Figure 8.- Continued.

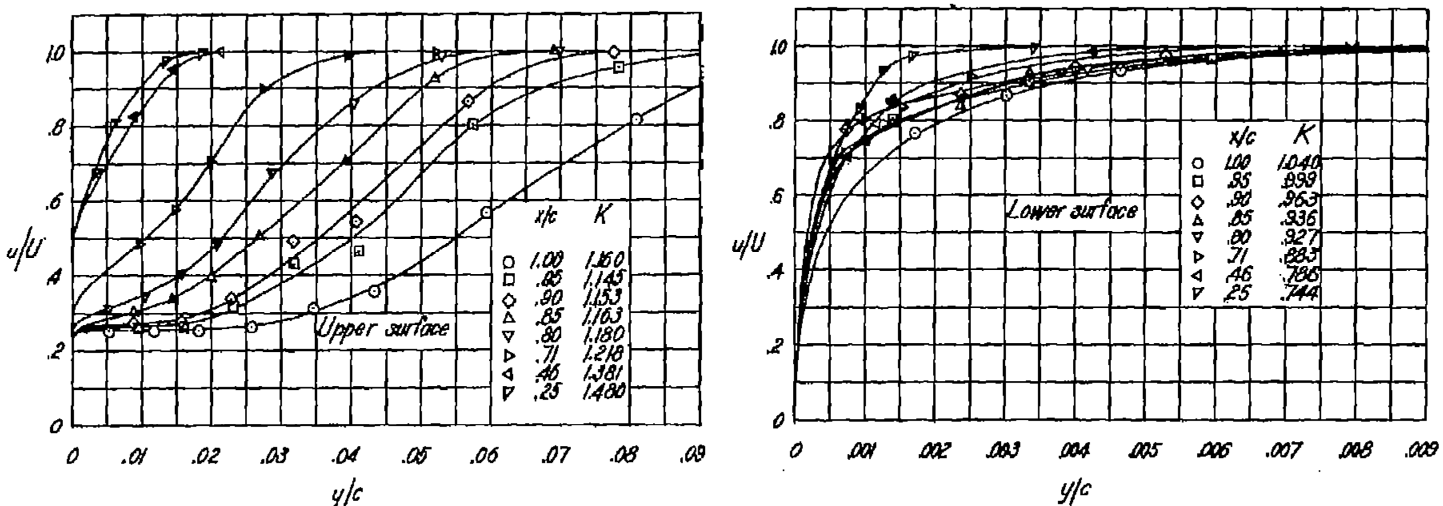

(j) $\alpha_0 = 8.3°$

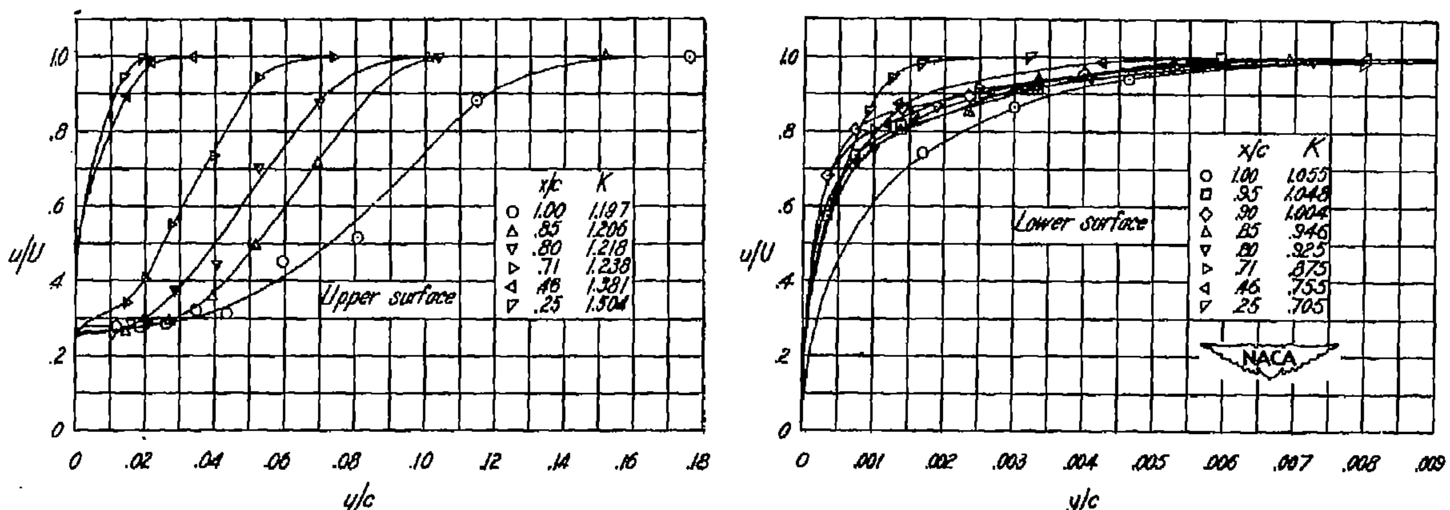

(k) $\alpha_0 = 10.3°$

Figure 8.— Concluded.

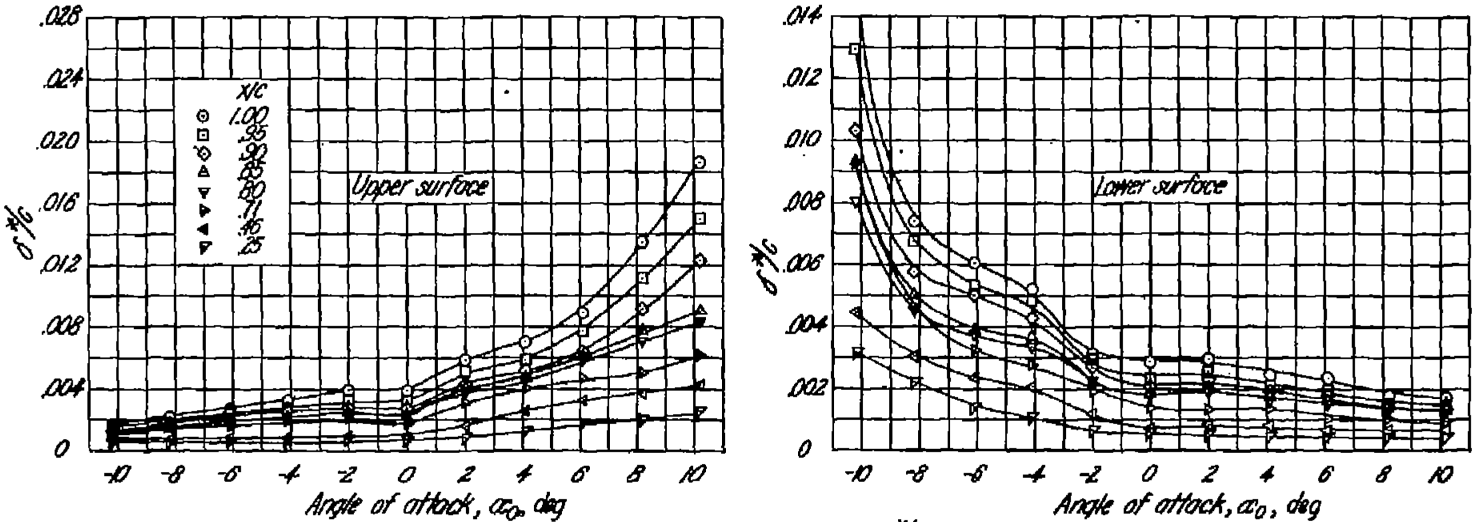

(a) Displacement thickness, δ^*/c.

NACA

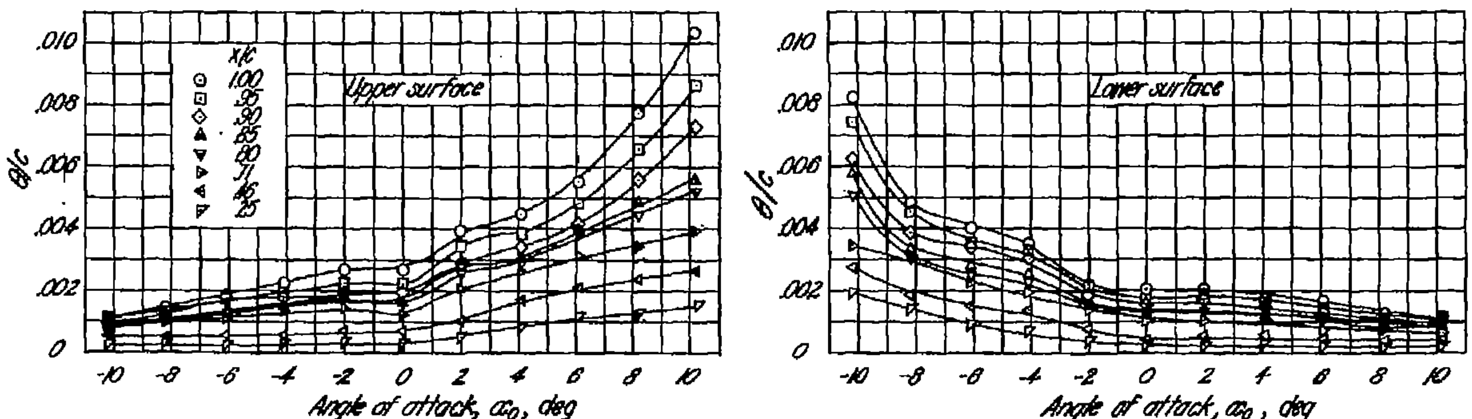

(b) Momentum thickness, θ/c.

Figure 9.- Boundary-layer parameters for NACA 0009 airfoil.

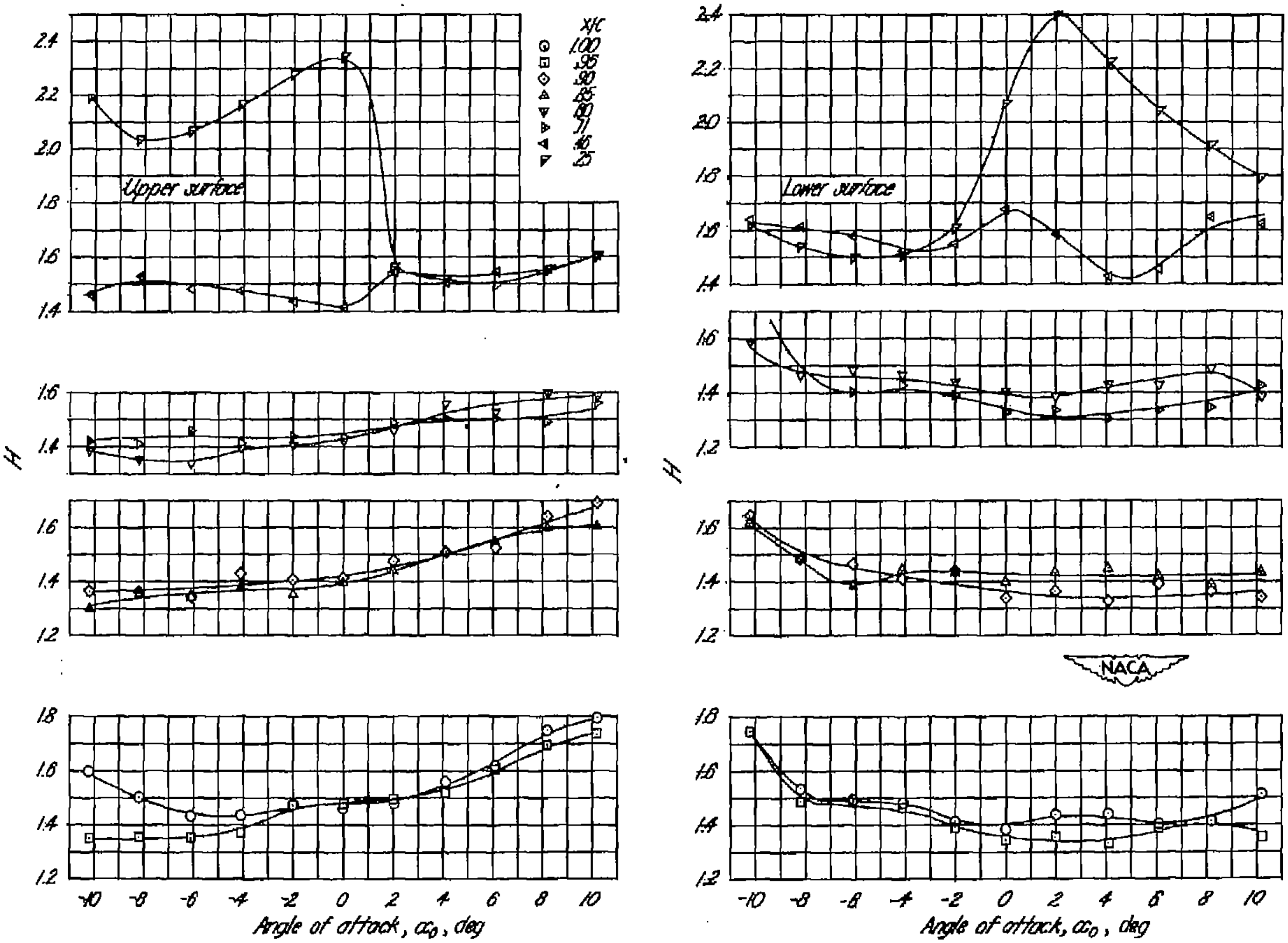

(c) Shape parameter, H.
Figure 9 - Concluded.

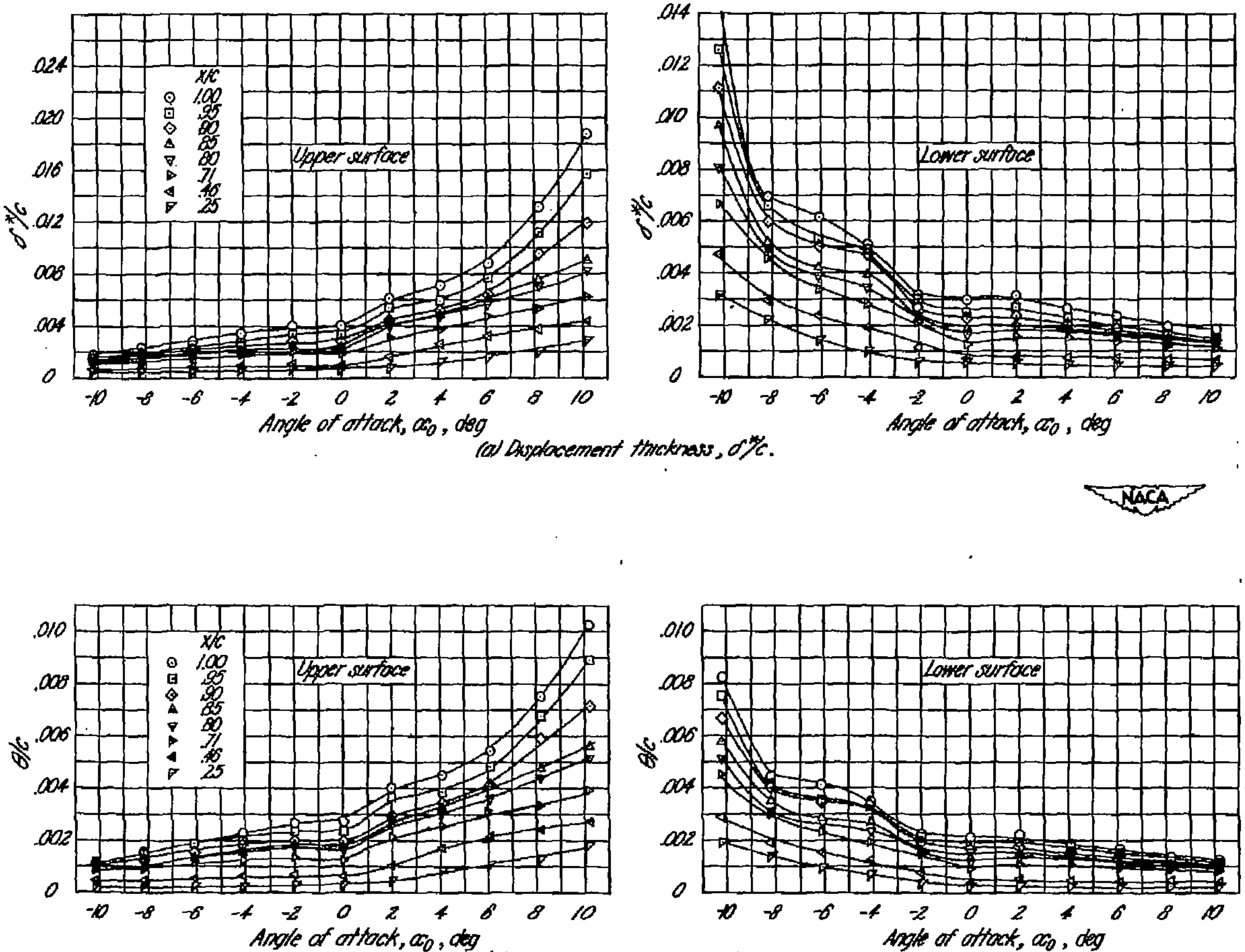

(a) Displacement thickness, δ*/c.

(b) Momentum thickness, θ/c.

Figure 10.- Boundary-layer parameters for NACA 0009 airfoil with 0.25c plain flap. δf = 0°.

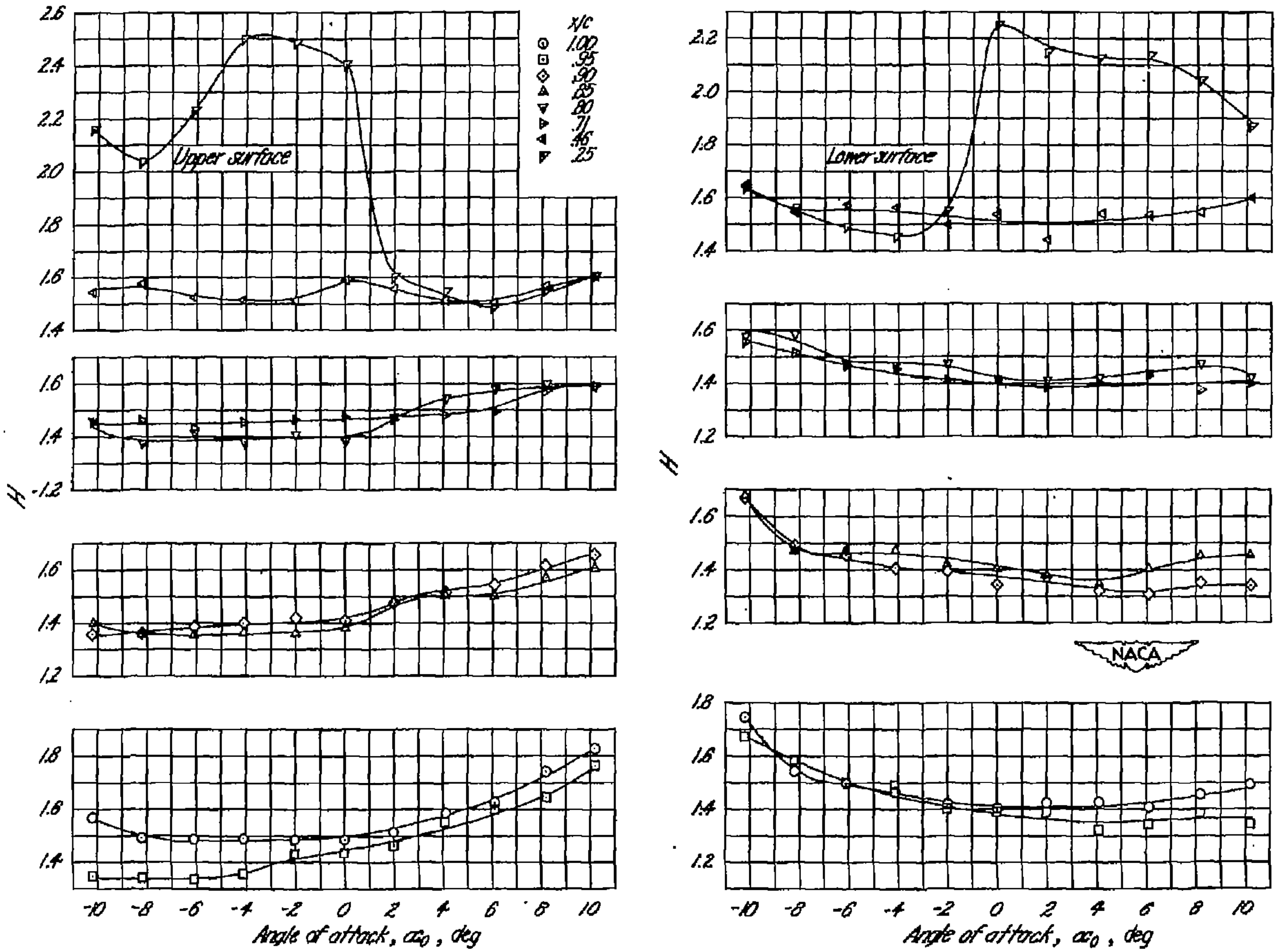

(c) Shape parameter, H.
Figure 10.- Concluded.

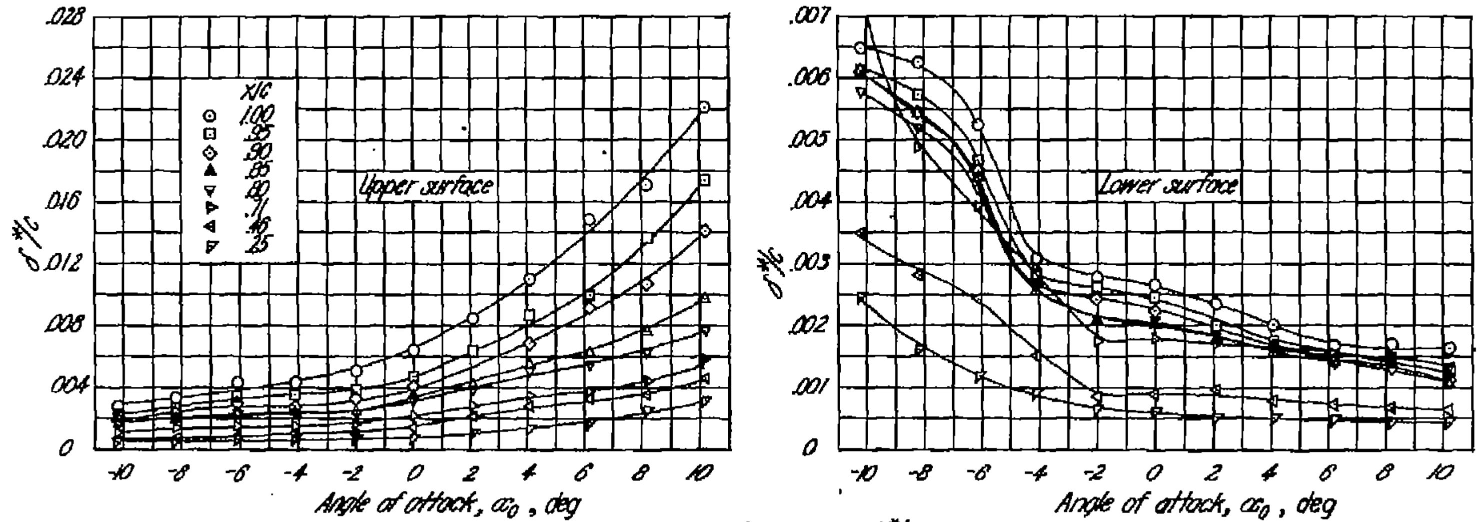

(a) Displacement thickness, δ^*/c.

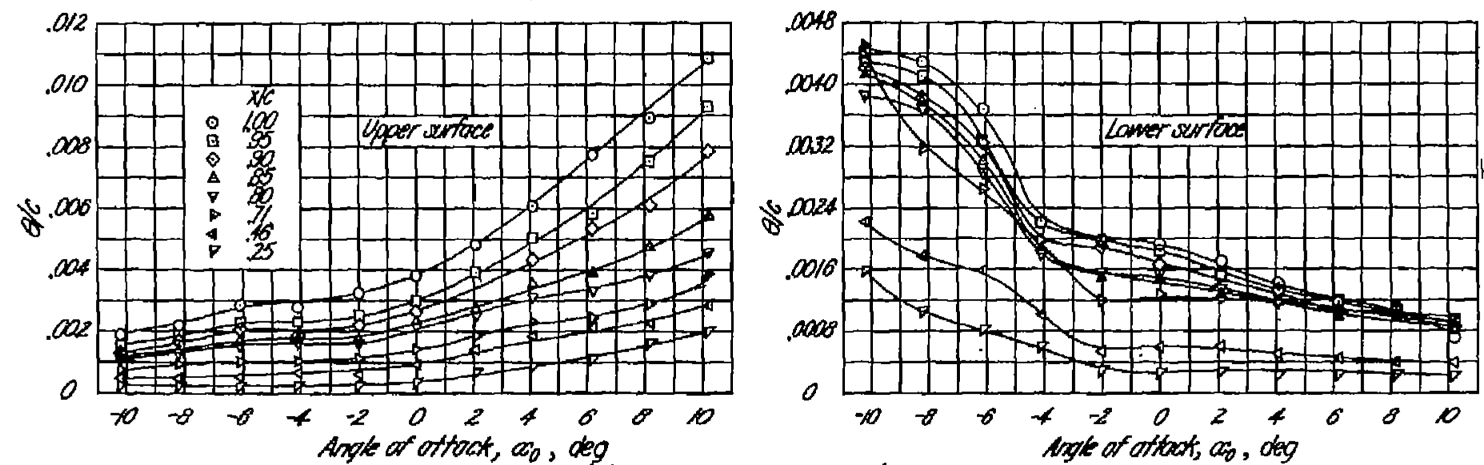

(b) Momentum thickness, θ/c.

Figure 11.- Boundary-layer parameters for NACA 0009 airfoil with 0.25c plain flap. $\delta_f = 5^\circ$.

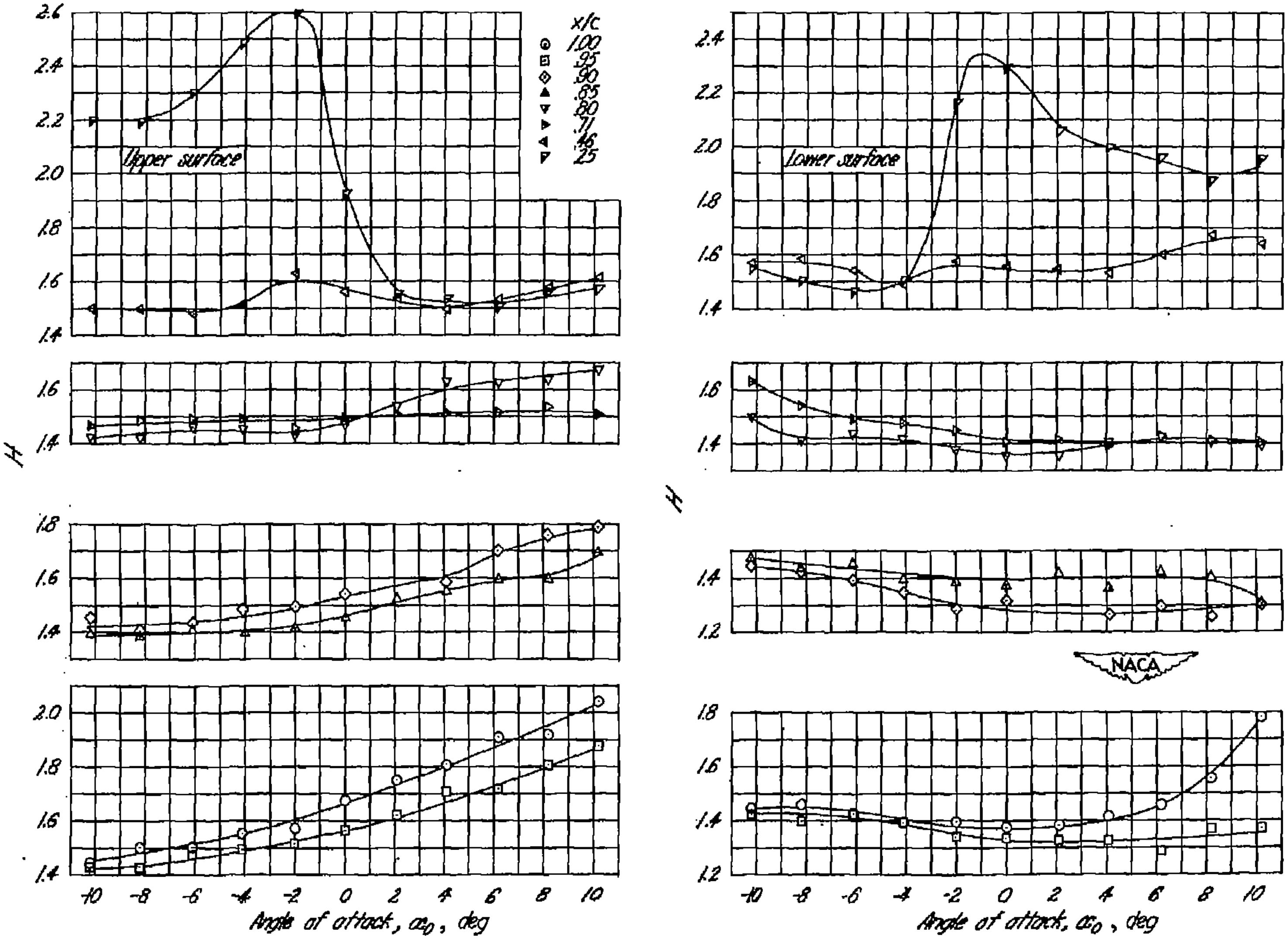

(c) Shape parameter, H.
Figure 11.- Concluded.

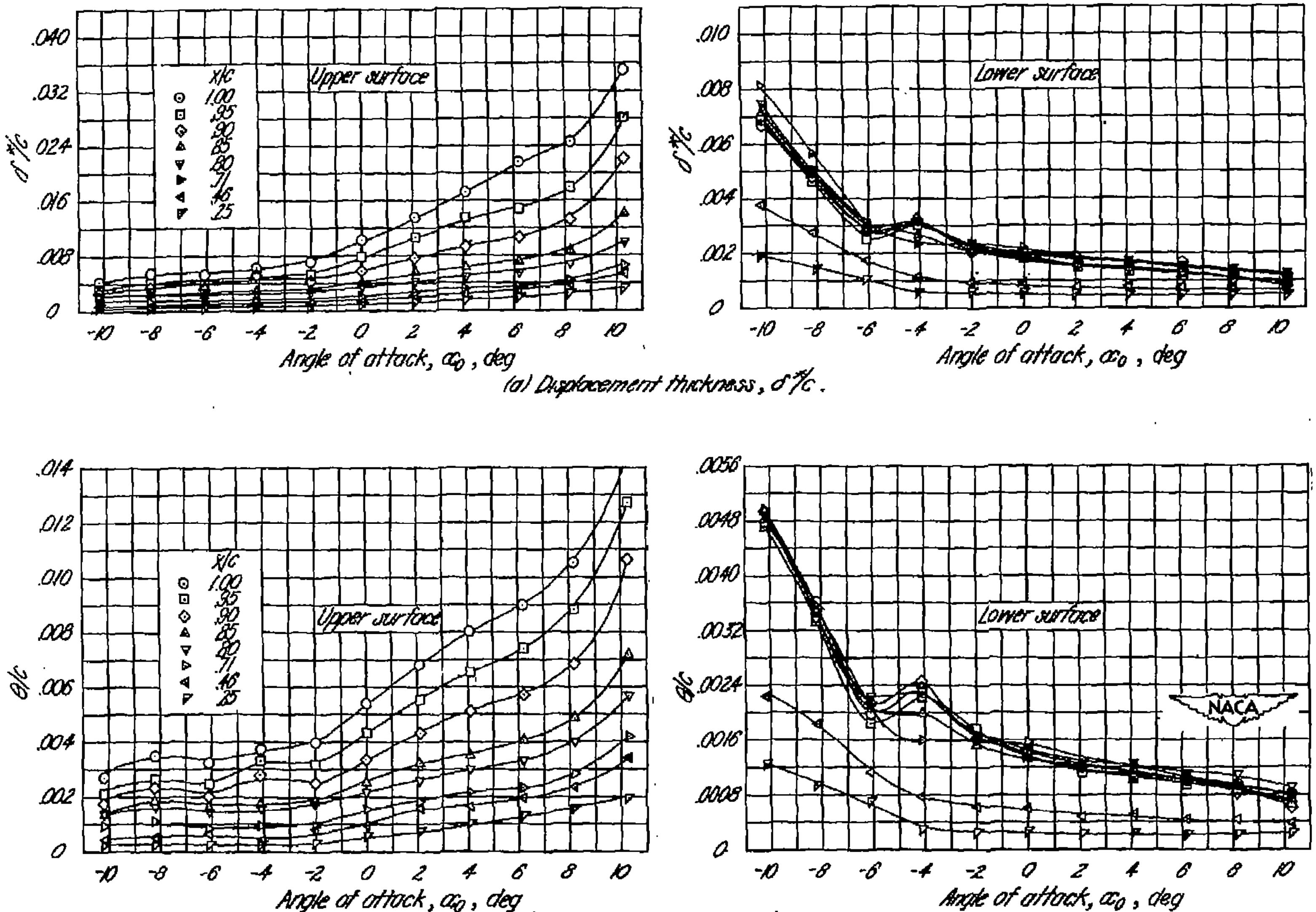

(a) Displacement thickness, δ^*/c.

(b) Momentum thickness, θ/c.

Figure 12.- Boundary-layer parameters for NACA 0009 airfoil with 0.25c plain flap. δ_f=10°.

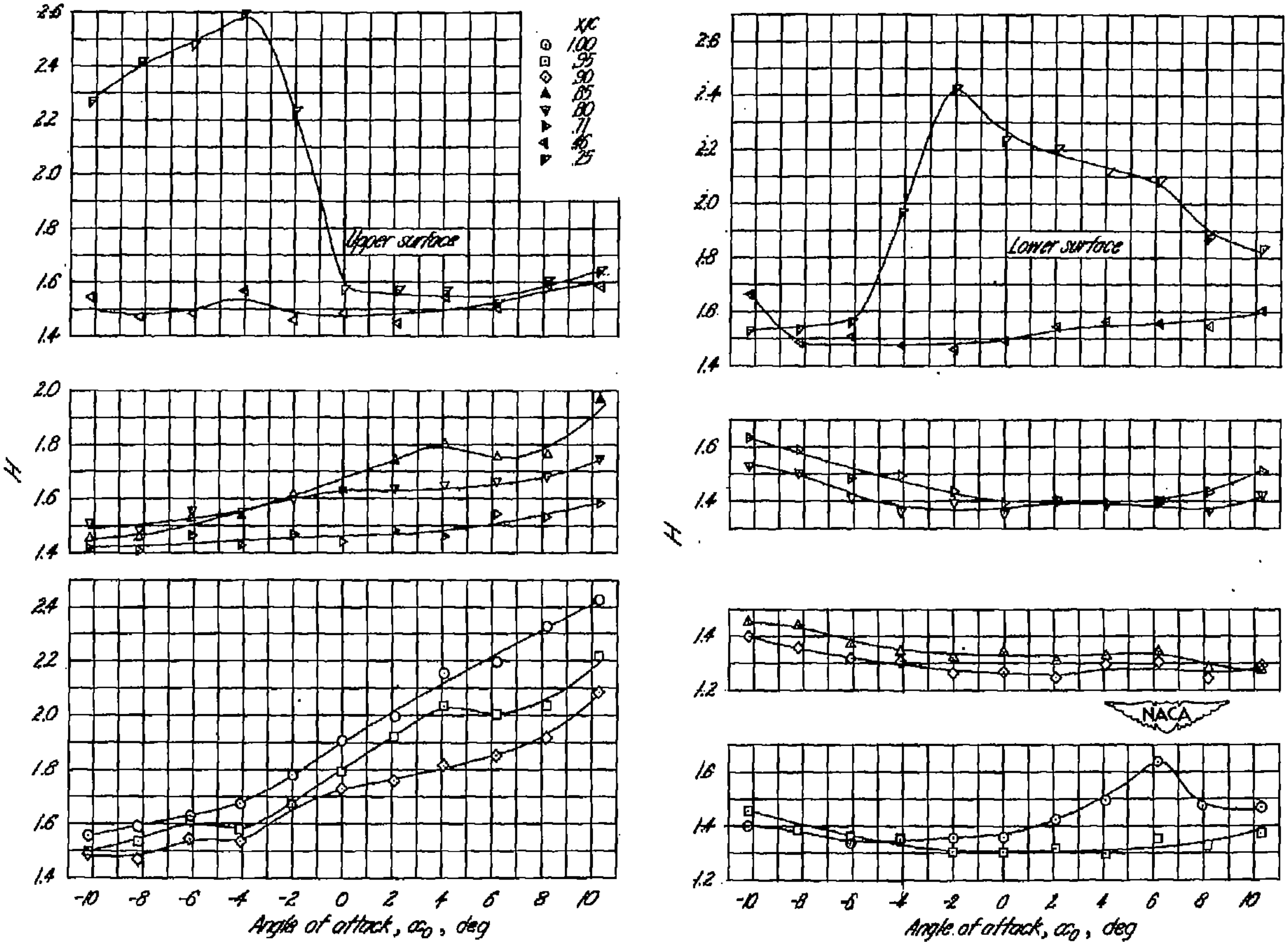

(c) Shape parameter, H.
Figure 12.- Concluded.

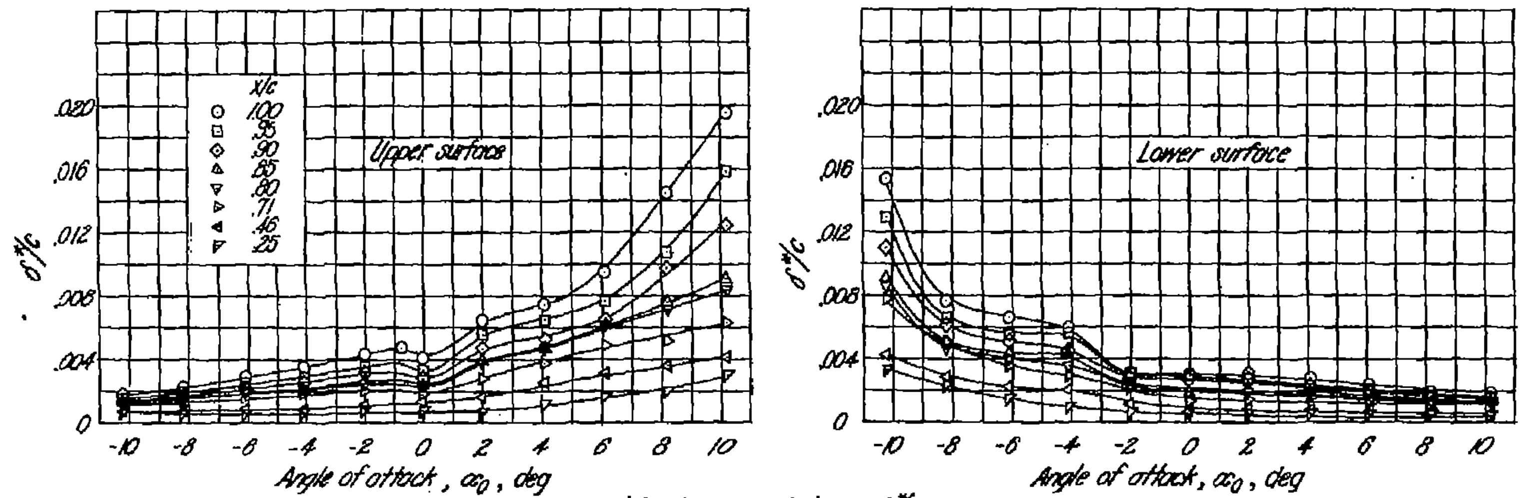

(a) Displacement thickness, δ*/c.

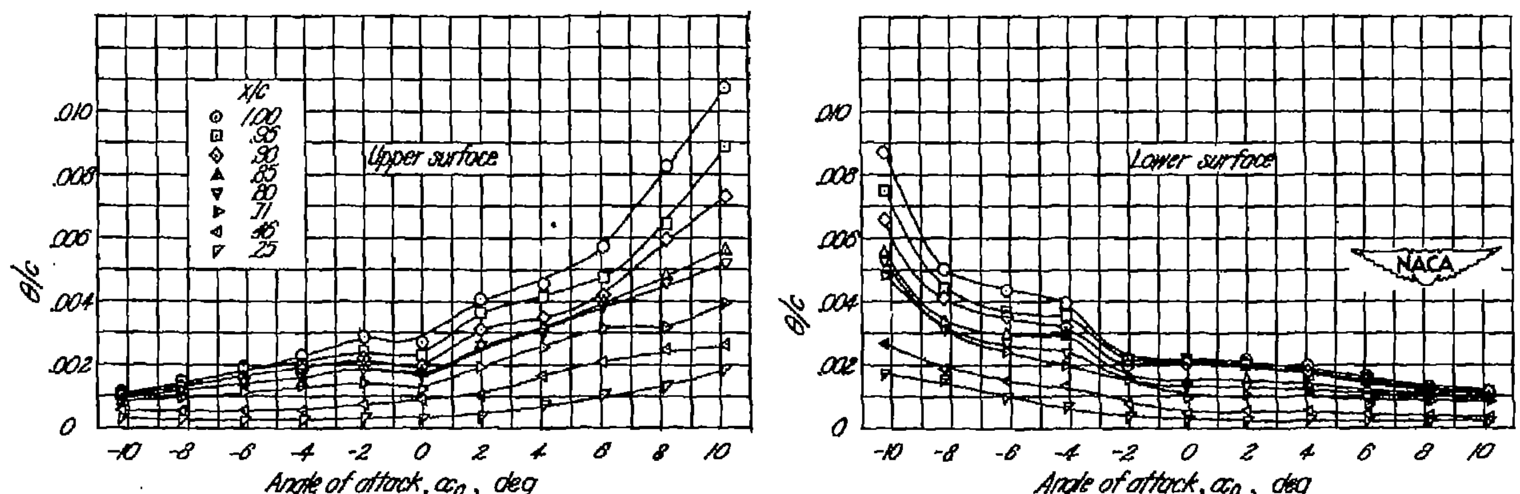

(b) Momentum thickness, θ/c.

Figure 13.- Boundary-layer parameters for NACA 0009 airfoil with 0.50c plain flap. $\delta_f = 0°$.

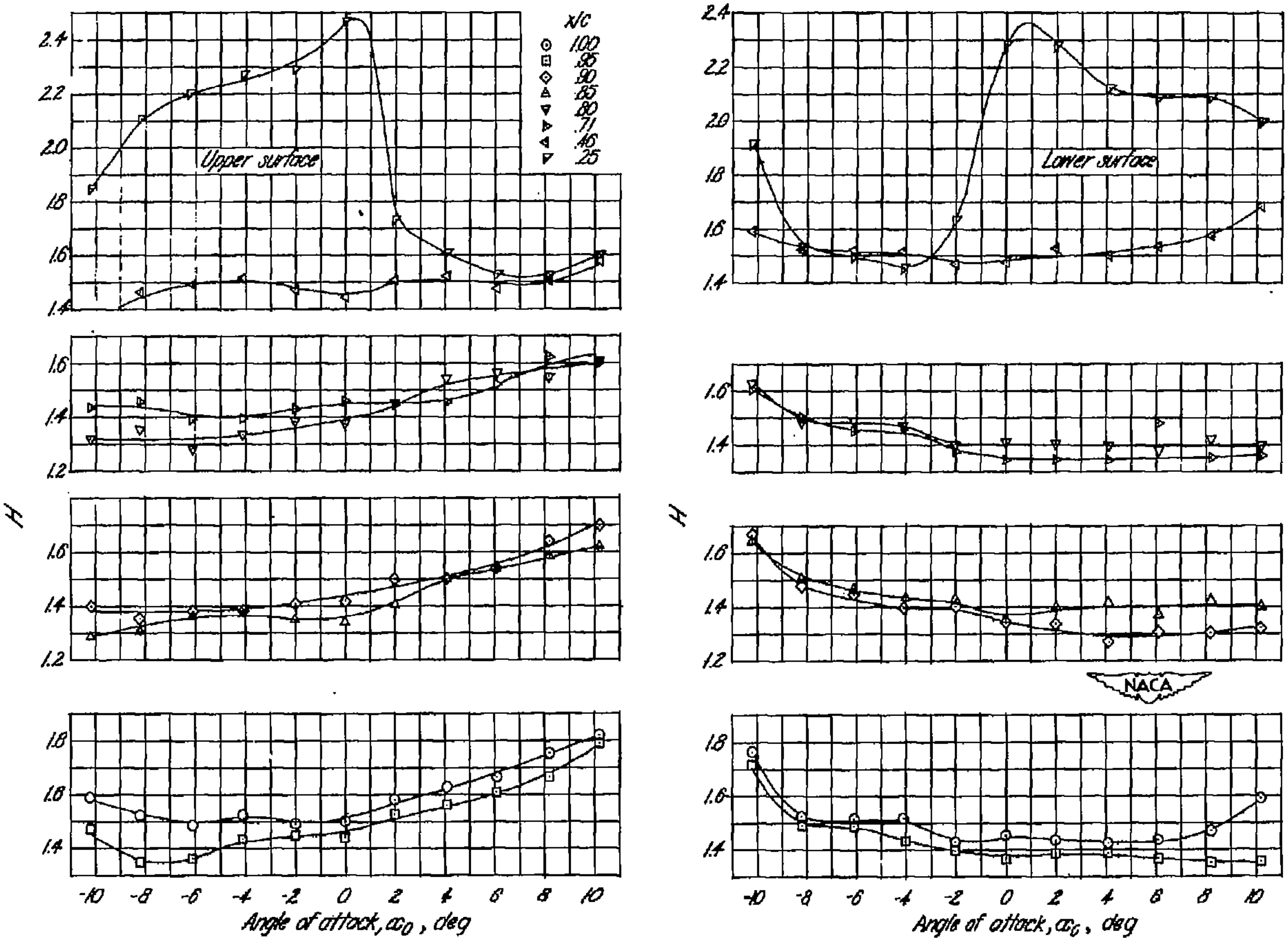

(c) Shape parameter, H.
Figure 13.- Concluded.

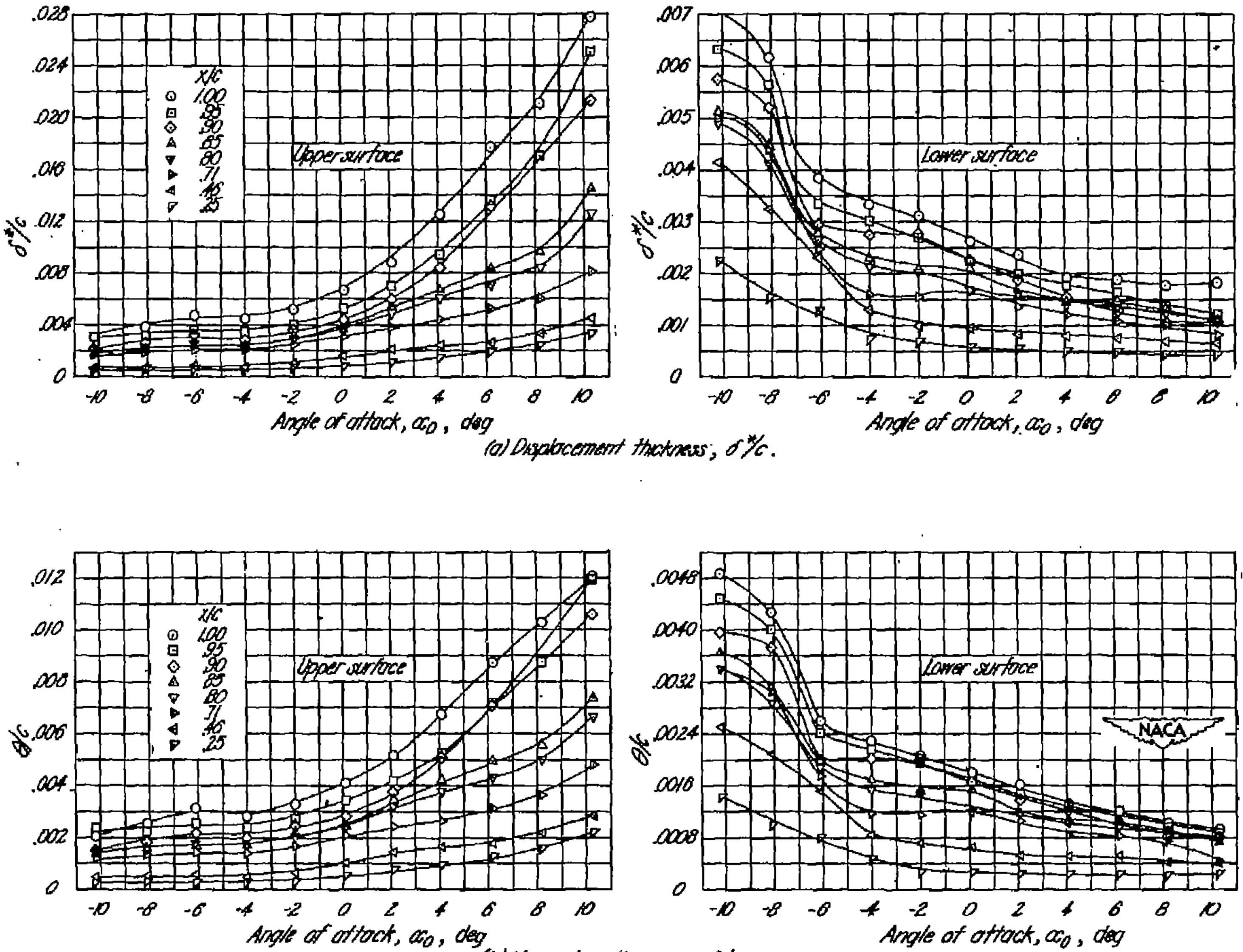

Figure 14.- Boundary-layer parameters for NACA 0009 airfoil with 0.50c plain flap. $\delta_f = 5°$.

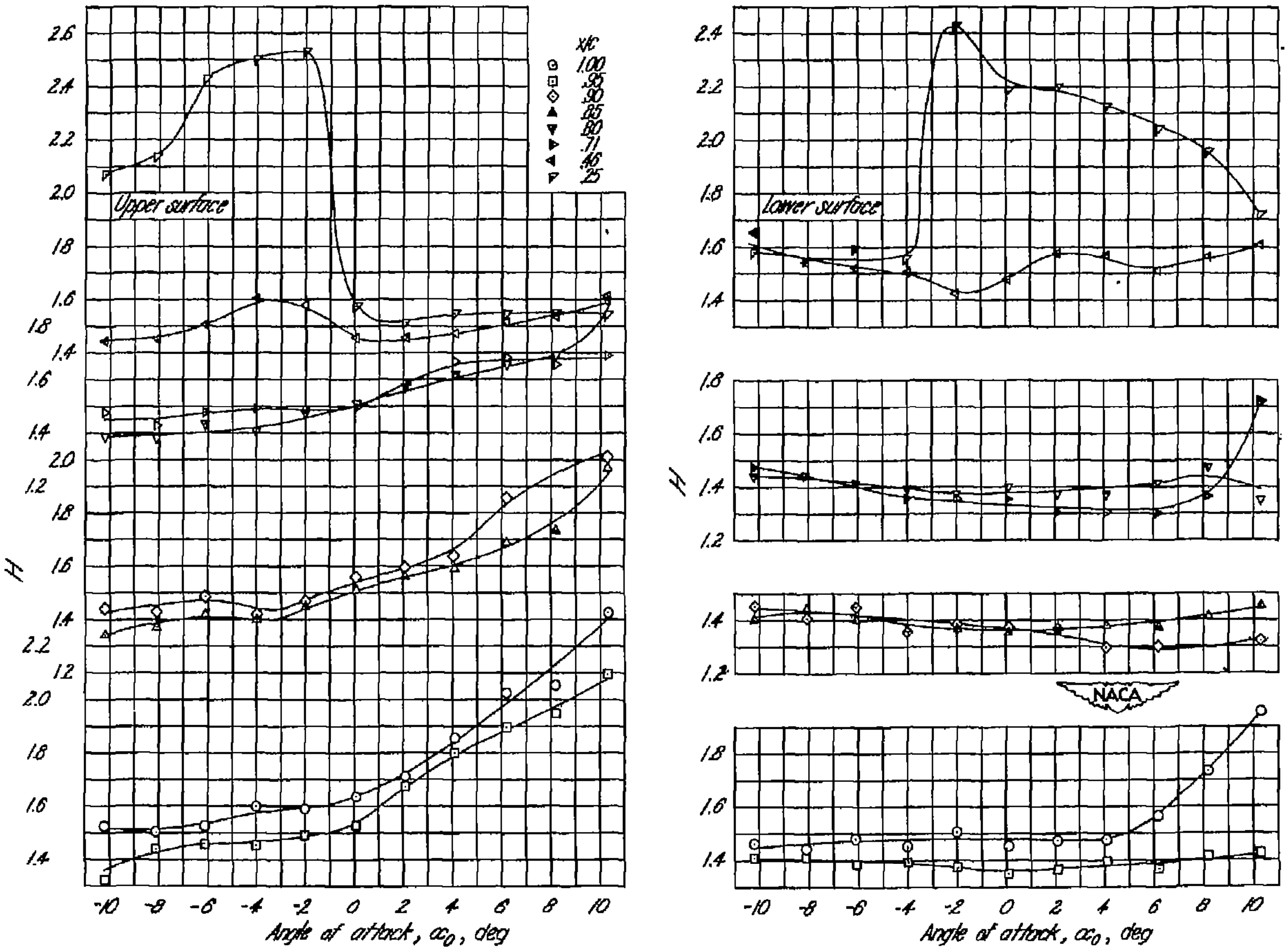

(c) Shape parameter, H.
Figure 14.- Concluded.

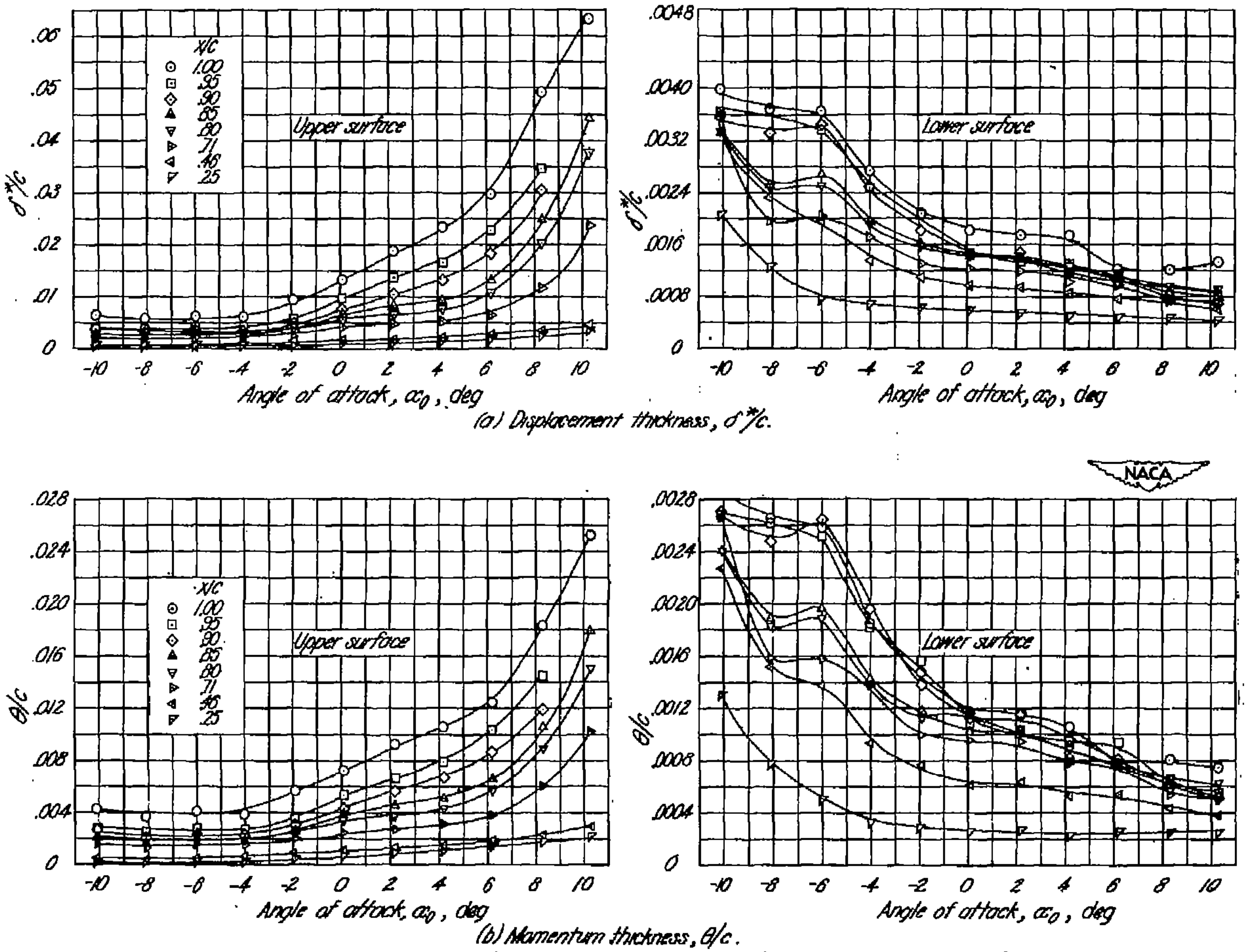

Figure 15.- Boundary-layer parameters for NACA 0009 airfoil with 0.50c plain flap; $\delta_f = 10^\circ$.

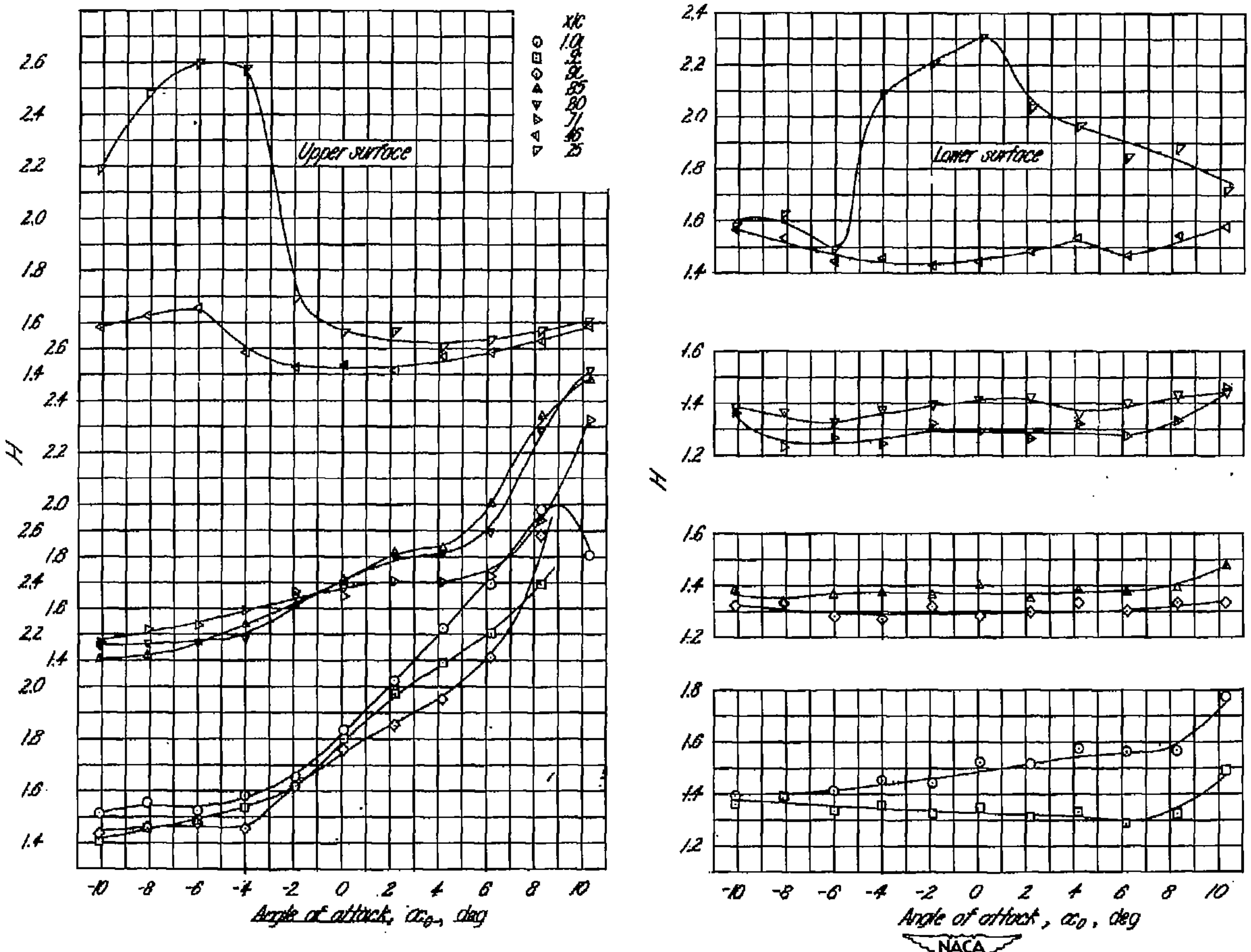

(c) Shape parameter, H
Figure 15.- Concluded.

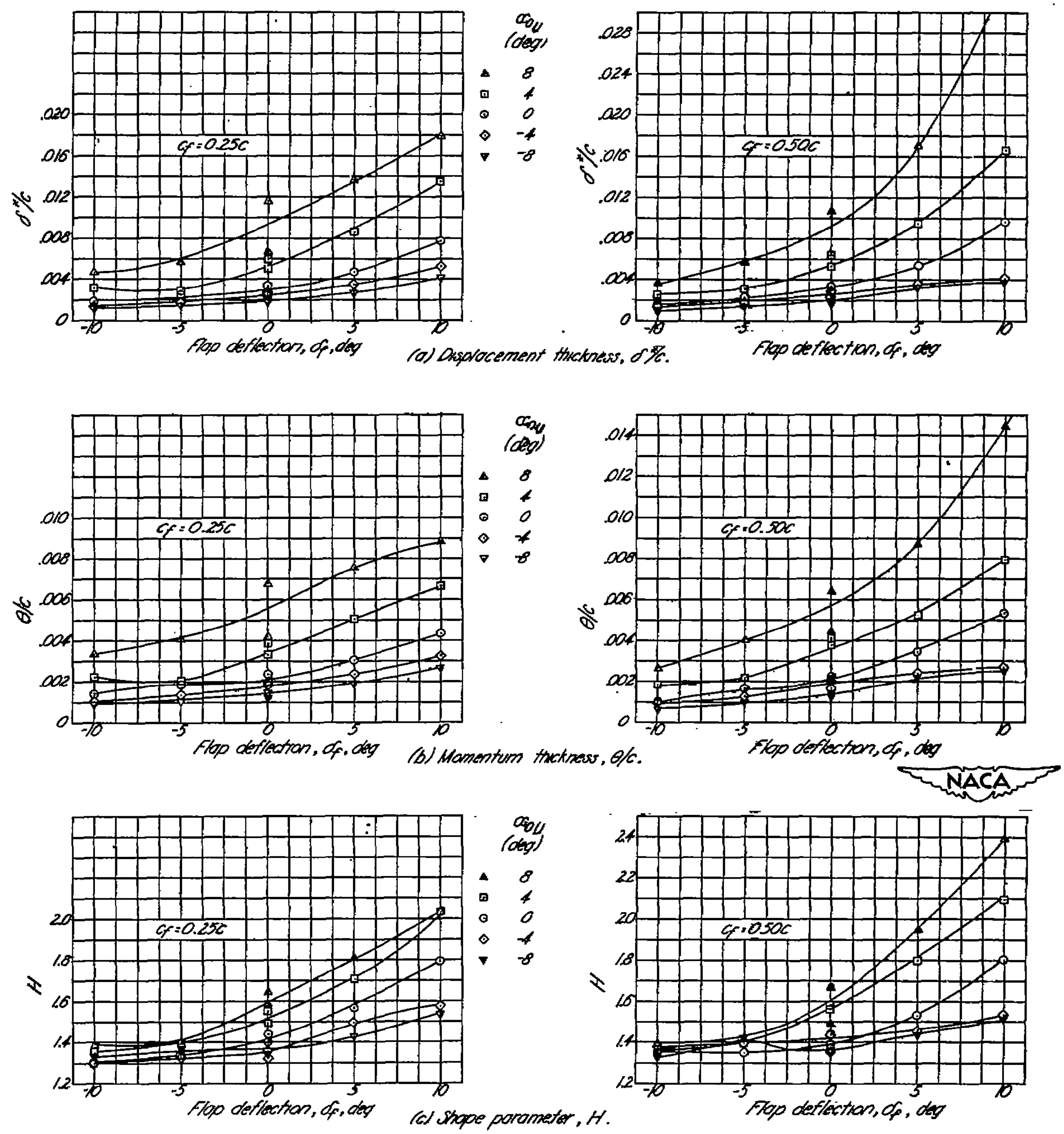

Figure 16.-Variation of boundary-layer parameters with flap deflection, upper surface. x=0.95c.

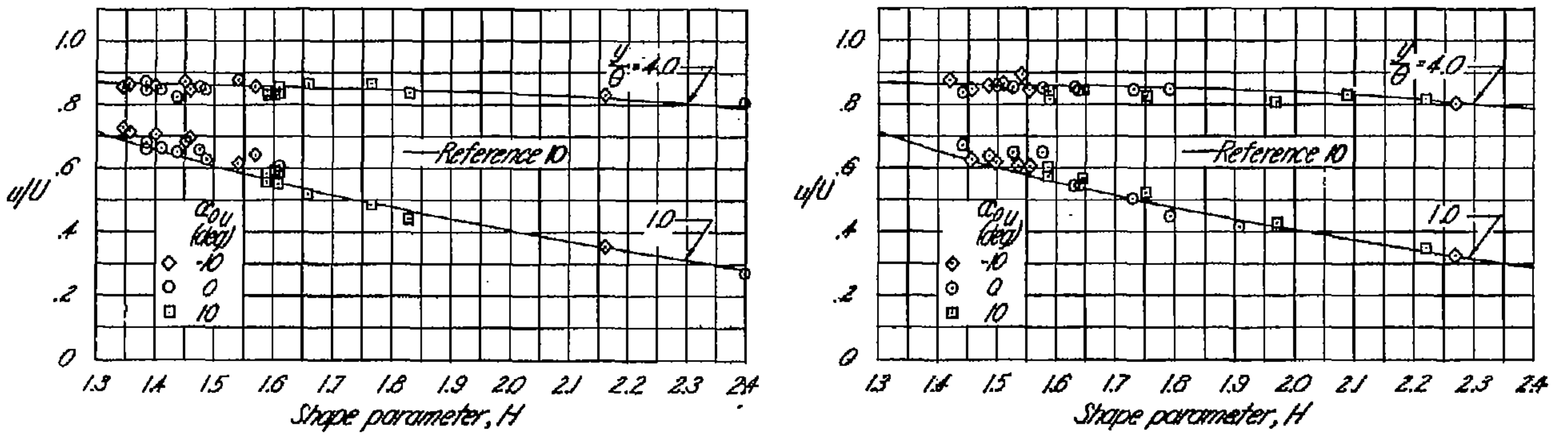

(a) $\delta_f = 0°$.

(b) $\delta_f = 10°$.

Figure 17.- Variation of u/U with H for NACA 0009 airfoil. $c_f = 0.25c$; $y/\theta = 1.0, 4.0$; upper surface.

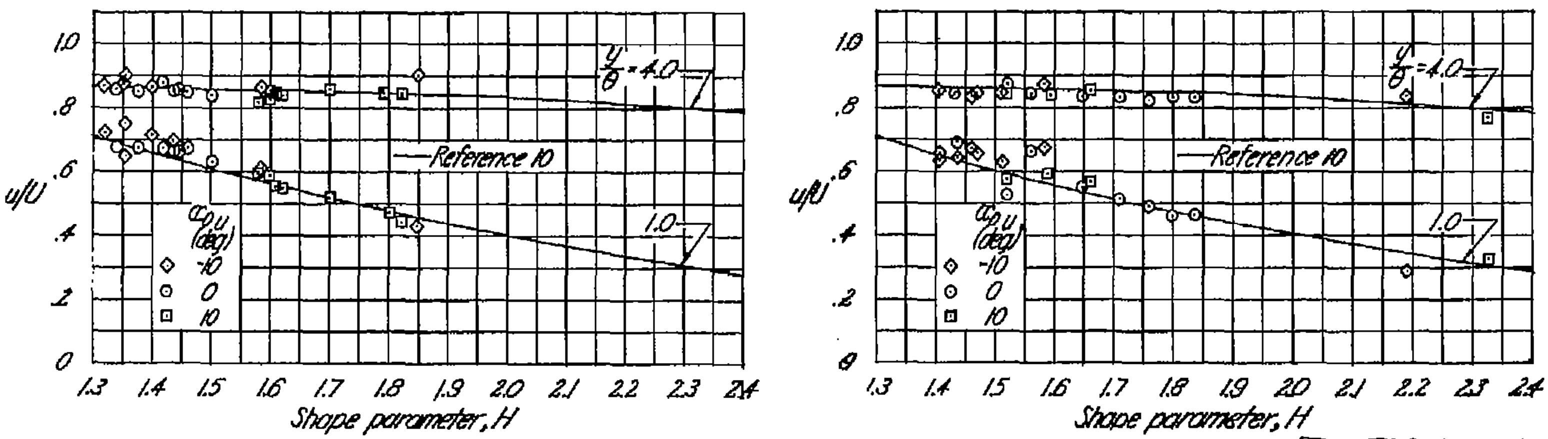

(a) $\delta_f = 0°$.

(b) $\delta_f = 10°$.

Figure 18.- Variation of u/U with H for NACA 0009 airfoil. $c_f = 0.50c$; $y/\theta = 1.0, 4.0$; upper surface.